RSC Advances

REVIEW

View Article Online
View Journal | View Issue

Cite this: *RSC Adv.*, 2021, **11**, 35472

Recent advances in functionalized upconversion nanoparticles for light-activated tumor therapy

Hongqian Chu,[ab] Tingming Cao,[ab] Guangming Dai,[ab] Bei Liu,[d] Huijuan Duan,[ab] Chengcheng Kong,[ab] Na Tian,[ab] Dailun Hou†*[c] and Zhaogang Sun†*[ab]

Upconversion nanoparticles (UCNPs) are a class of optical nanocrystals doped with lanthanide ions that offer great promise for applications in controllable tumor therapy. In recent years, UCNPs have become an important tool for studying the treatment of various malignant and nonmalignant cutaneous diseases. UCNPs convert near-infrared (NIR) radiation into shorter-wavelength visible and ultraviolet (UV) radiation, which is much better than conventional UV activated tumor therapy as strong UV-light can be damaging to healthy surrounding tissue. Moreover, UV light generally does not penetrate deeply into the skin, an issue that UCNPs can now address. However, the current studies are still in the early stage of research, with a long way to go before clinical implementation. In this paper, we systematically analysed recent advances in light-activated tumor therapy using functionalized UCNPs. We summarized the purpose and mechanism of UCNP-based photodynamic therapy (PDT), gene therapy, immunotherapy, chemotherapy and integrated therapy. We believe the creation of functional materials based on UCNPs will offer superior performance and enable innovative applications, increasing the scope and opportunities for cancer therapy in the future.

Received 23rd July 2021
Accepted 28th October 2021

DOI: 10.1039/d1ra05638g

rsc.li/rsc-advances

1. Introduction

Due to increasing lifespans, sedentary lifestyles and unhealthy eating habits, cancer has become a major public health problem of global proportions. Statistics have shown that over 18 million new cancer cases occurred worldwide in 2018, with a reported mortality of 9.6 million.[1] In spite of vast investments in emerging cancer treatment technologies, cancer morbidity and mortality remain stubbornly high. Present conventional cancer treatments (*e.g.* chemotherapy, immunotherapy, radiotherapy) have demonstrated only modest clinical success due to low drug delivery efficiency and the emergence of multi-drug resistance (MDR).[2–4] Moreover, emerging treatments have demonstrated significant toxic side effects.[3,4] Nanomaterials are considered a promising medium for medical applications such as drug delivery and targeted cancer therapy due to their high surface-to-volume ratio and the ability to penetrate deep into tissues or cross-membrane barriers.[5,6] In recent decades, the development of much safer and more reliable nanoscale drug delivery systems for successful cancer therapy has been pursued vigorously due to their potential to improve effectiveness and enable precise cancer targeting.

To date, various nanoscale pharmaceutical carriers have been investigated in terms of possible cancer therapies, including liposomes, high molecular weight polymers, carbohydrates (*e.g.* carbon nanotubes, graphene oxide), mesoporous silica, magnetic nanoparticles, gold nanoparticles and other nanoparticles.[7,8] Even though therapeutic drugs can be delivered by a nanoscale drug carrier to the tumor due to the phenomenon of local increased permeability and retention (EPR) at the tumor site, premature drug release can trigger organ damage and reduce the efficiency of drug release inside tumor cells, thus decreasing the therapeutic effectiveness,[9,10] which significantly hindered clinical applications. The exploration of new nanoscale systems with targeted and controllable drug-release profiles is urgently needed to tackle the above-mentioned poor effectiveness and poor supply quality.[11–14]

Controlled activation or release of biomolecules is crucial for many different biological applications. Various methods were used to track the behaviour of biomolecules, and light-induced activation has gained popularity in recent decades. The key obstacle in this process is that photo-activated compounds mainly react to ultraviolet (UV) and not to visible or near-infrared (NIR) light. Upconversion nanoparticles (UCNPs) are a unique class of lanthanide-doped optical nanocrystals.[15,16] UCNPs can transform two or more low-energy pump photons from the NIR to a higher-energy photon with a shorter wavelength,[17–20] which has drawn considerable interest in many

[a]*Translational Medicine Center, Beijing Chest Hospital, Capital Medical University, Beijing 101149, PR China. E-mail: sunzhaogang@bjxkyy.cn*

[b]*Beijing Key Laboratory in Drug Resistant Tuberculosis Research, Beijing Tuberculosis and Thoracic Tumor Research Institute, Beijing 101149, PR China*

[c]*Department of Radiology, Beijing Chest Hospital, Capital Medical University, Beijing, 101149, PR China. E-mail: houdailun@163.com*

[d]*School of Science, Minzu University of China, Beijing 100081, PR China*

† These authors contributed equally to this work.

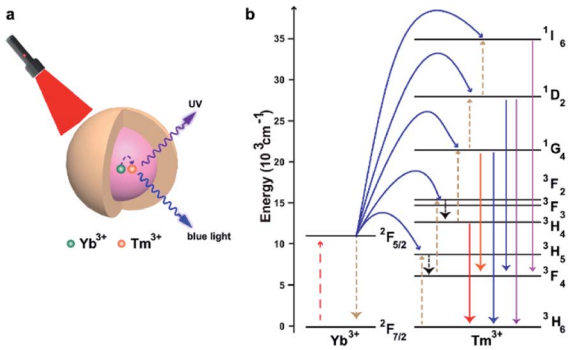

Fig. 1 (a) Illustration of the energy transfer mechanism of the core–shell NaGdF4:Yb/Tm@NaGdF4 UCNPs. The energy transfer occurs through the Yb → Tm pathway upon 980 nm excitation. (b) Energy level diagrams of the Yb^{3+} and Tm^{3+} ions and the energy transfer mechanism of the UCNPs in the energy level.

fields, including biomedicine. The mechanism of upconversion luminescence (UCL) has been identified and was developed for applications in biosensing, imaging and therapy, especially in oncology.[21–24] Fig. 1 shows NaGdF4:Yb/Tm@NaGdF4, a typical example of a UCNP with a core–shell structure. These UCNPs exhibited characteristic UCL bands at 313, 363, 453, and 478 nm upon 980 nm CW laser excitation.[25] Due to the unique optical properties of UCNPs, they can be designed and modified to achieve effective drug delivery and release guided by a specific stimulus. Several NIR-responsive drug delivery systems based on UCNPs have been successfully developed, offering great promise for effective cancer treatment using UCNPs as efficient NIR light transducers to activate therapeutics that react to visible or UV light. Here, we mainly discuss recent advances in functionalized UCNPs for light-activated tumor therapy.

In this review, we aim to provide a landscape of the strategies of using UCNPs for light-activated tumor therapy. We underline the four UCNPs-based tumor therapy methods and the agents that play key roles in material fabrication.

2. Upconversion-based photodynamic therapy

Due to its non-invasive nature and spatiotemporal accuracy, light-induced therapy is a powerful strategy for localized precision therapy. Photodynamic therapy (PDT) is a clinical treatment method that incorporates light, photosensitizers (PSs), and reactive oxygen species (ROS) to treat cancers and non-malignant diseases.[26–28] As shown in (Fig. 3), Compared to traditional chemotherapy and radiation therapy, PSs only works at the light-irradiated site, dramatically reducing systemic toxicity.[29] However, the low water solubility and poor tumor selectivity of PSs has seriously impeded their clinical use.[30,31] In particular, the phototoxicity of light and nonspecific activation of singlet oxygen production in normal tissues has also resulted in prolonged photosensitivity of the skin or eyes, thereby limiting the utility of PSs as therapeutic agents.[32–34] In addition to the above-mentioned drawbacks of PDT, the low tissue penetration of light used in the clinic for activating PSs is another significant drawback.[35] Thus, methods for spatially selective antitumor activation are urgently needed. Because of their unique optical properties, UCNPs are a great option to solve the above problems. Moreover, a series of strategies, such as physical adsorption, covalent conjugation and silica encapsulation, have been utilized for loading UCNPs with PSs.[36]

2.1 Physical adsorption of PSs for PDT

Physical adsorption is a process for the modification of nanomaterials that is based on non-covalent binding between hydrophobic PS and the hydrophobic layer on the surface of UCNPs.[37,38] Chatterjee and Yong constructed a nanomaterial by using zinc phthalocyanine (ZnPc) to attach PEI-modified UCNPs, which was used as a nano transducer for PDT and showed a strong tumor cell killing effect.[39] Zhuang's group carried out some creative work on non-covalent physical adsorption.[7,40,41] They modified UCNPs using an amphiphilic polymer derived from polyethylene glycol (PEG) that can provide excellent water-solubility for PEGylated UCNPs. PEGylation can improve the stability and minimize the toxicity of the UCNP-PS complex, while the hydrophobic oleic-acid layer on the surface above and below the PEG coating enables the adsorption of the hydrophobic PSs molecules chlorine 6 (Ce6) for successful drug loading (Fig. 2). The strategy is rather straightforward without further modification, and the thickness of the hydrophobic layer is less than 5 nm, and not 30 nm as in previous reports. Thus, the short distance between UCNPs and Ce6 molecules results in energy resonant transfer from UCNPs to Ce6.[7]

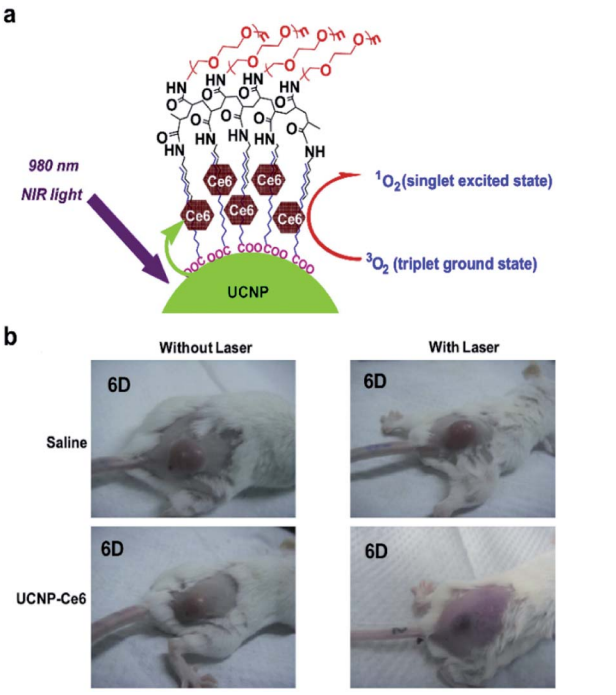

Fig. 2 (a) Scheme of Ce6 physically adsorbed on the surface of PEGylated UCNPs *via* hydrophobic interactions to form UCNP-Ce6 complex. (b) Representative photos of mice after various treatments indicated at the 6th day.[7]

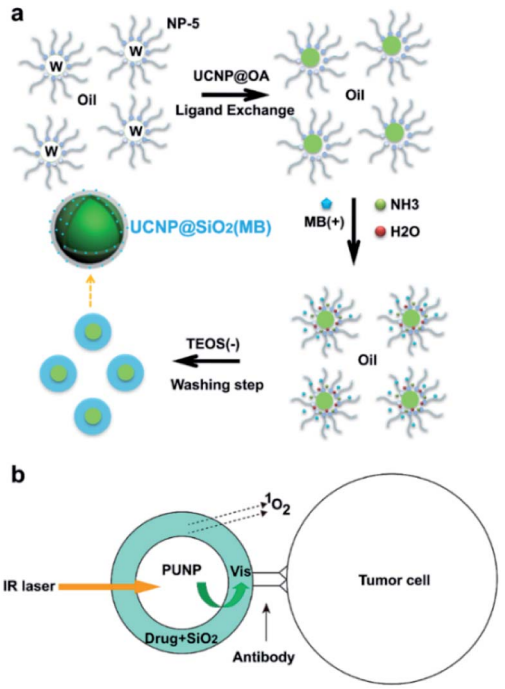

Fig. 3 (a) The formation mechanism of $NaYF_4$:Er/Yb/Gd@SiO_2 (MB) in the water-in-oil reverse microemulsion system.[59] (b) Schematic of the design of the versatile photosensitizer based on photon upconverting nanoparticles.[58]

2.2 Silica encapsulation for PS delivery

Mesoporous silica nanoparticles (MSNs) are synthesized using self-assembled surfactant molecules as condensation templates for silica precursors, followed by the removal of the template material to leave a rich network of cavities.[42,43] This new family of materials features organized pore dispersion, tailored pore sizes, large surface area and high density of silanol at the surface, making MSNs a perfect carrier for loading a large amount of molecules.[44–50] MSNs have received significant attention in the past and have been explored as effective carriers for a variety of therapeutic agents against different diseases, including cancer.[51–55]

UCNPs coated with porous silica have become an appealing drug delivery system that combines a light conversion property with a high loading capacity, enabling the physical encapsulation of payload molecules and achieving light-triggered drug release and activation.[56,57] Zhang *et al.*[58] as well as Shi *et al.*[59] reported the first attempts to mechanically encapsulate PS molecules using silica-coated UCNPs for PDT (Fig. 3). The encapsulation was conducted in the solution in both cases, so that the negative charge and hydrophilic properties of the silicate layer together with the hydrophobic photosensitizer showed an unfavorable encapsulation effect, which resulted in a low efficiency of PS loading and leakage of PS from the particle surface.[58] Another loading strategy developed for UCNP-based delivery systems is physical adsorption *via* electrostatic attraction.[60–63]

Recent advances in UCNPs involving co-loaded anticancer drugs (DOX) and chlorine Ce6 with high antitumor effectiveness have showed great promise in the manufacturing of bifunctional materials (pH- and ROS-responsive). As shown in (Fig. 4), on the surface of UCNPs@$mSiO_2$, DOX and Ce6 were conjugated and prepared. The average size of UCNPs@$mSiO_2$ after loading DOX and Ce6 was 85.63 ± 9.87 nm. The resulting UCNPs@$mSiO_2$ had a small size (<100 nm) for further loading of drug and PS, which yields a photo-induced drug delivery system and may boost the cell uptake and activate Ce6, which regulated the release of DOX by 980 nm NIR irradiation.[64]

The authors also developed a mesoporous silica-coated UCNP system in which photochemically incorporated porphyrin PSs and NIR-responsive diarylethene (DAE) photochromic switches are loaded into nanopores. The UCNP core absorbs low-energy photons when irradiated with 980 nm NIR light. It transfers energy to the silica walls and efficiently produces $^1O_2$. This 980 nm NIR light-sensitized behaviour can also be controlled remotely by 808 nm light irradiation. In the closed form of the DAE mounted in the nanopores, $^1O_2$ generation is inhibited, while after irradiation with 808 nm NIR light, the DAE is transformed into an open shape, thus enhancing the 980 nm NIR production of $^1O_2$ (Fig. 5). Also, the outer shell thickness of <3 nm further enhances the efficiency of resonance energy transfer between UCNPs and PSs. The NIR on-demand light-mediated nanoarchitecture activations has great advantages for the efficient delivery of an integrated photosensitive system in living cells that allows for *in vitro* and *in vivo* activation of PDT with efficient control of $^1O_2$ release.[65] The loading of

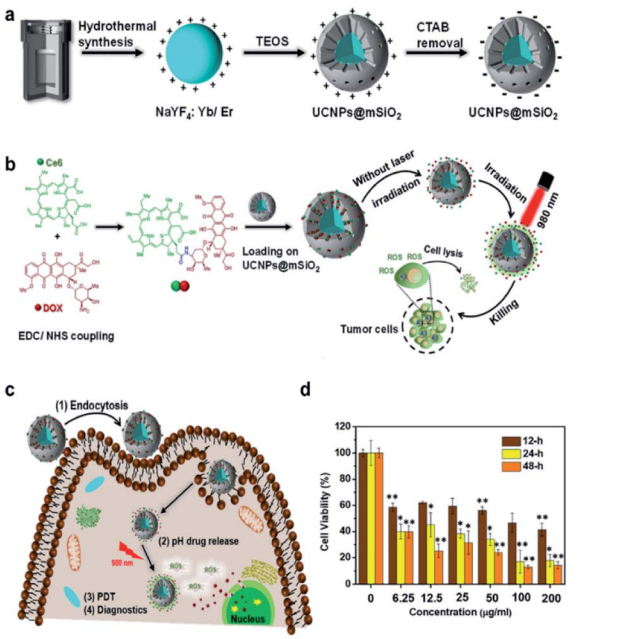

Fig. 4 (a) Schematics of the UCNPs and UCNPs@$mSiO_2$. (b) Preparation and characterization of DOX/Ce6 conjugates and loading on the surface of UCNPs@$mSiO_2$. (c) Schematic of the mechanism of the NP internalization and combined pH drug release and PDT effects under the NIR light exposure. (d) Relative viabilities of the cancer cell lines incubated for various times with different concentrations of UCNPs@$mSiO_2$-DOX/Ce6 exposed to the 980 nm laser (0.45 W cm^{-2}, 10 min).[64]

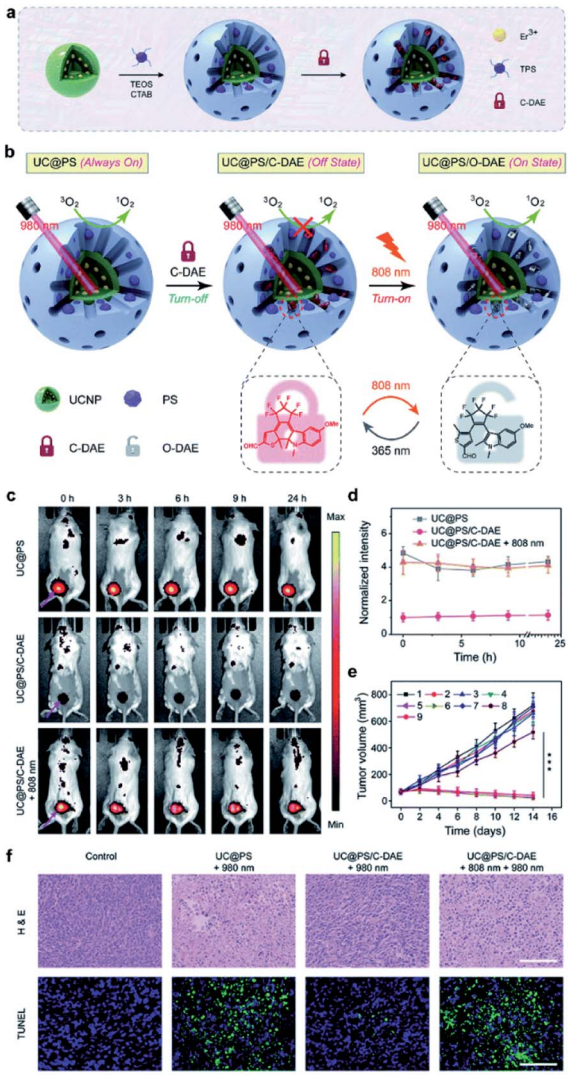

Fig. 5 (a) Schematic showing the synthesis procedure of UC@PS/C-DAE. (b) Schematic illustration of the 980 nm NIR light photosensitized UC@PS/C-DAE nanoconstruct, whose 1O2 generation capability can be remotely switched on by 808 nm NIR light irradiation. (c and d) Representative time-dependent *in vivo* fluorescence imaging of 4T1 tumor-bearing mice after exposure to different treatments. (e) The 4T1 tumor growth curves after different treatments. (f) Histological images of the tumor sections on day 14 post various treatments. The tissues were stained with H&E and TUNEL, respectively.[65]

PSs in the pores of mesoporous silica may enhance its stability in the complicated cell microenvironment compared to a solid silica sheet and contribute to a faster generation and release of $^1O_2$ in the target tissue.

The rapid growth of tumor cells requires large amounts of oxygen, leading to a hypoxic tumor microenvironment, which is an undesirable condition in the tumor that drastically reduces the efficacy of PDT.[66–68] As shown in (Fig. 6), Liu *et al.* constructed new UCNPs named TPZ-UC/PS, which have a co-delivery capacity for PSs and the prodrug tirapazamine (TPZ) which can be activated and becomes extremely toxic under hypoxic conditions.[69] This is an effective synergetic PDT/chemo-

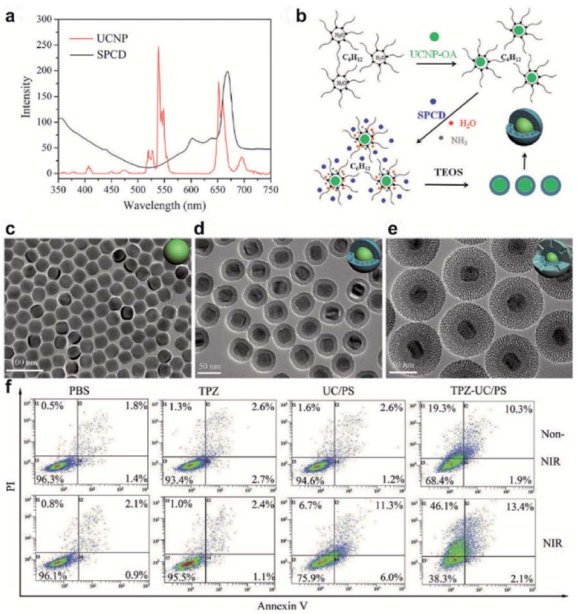

Fig. 6 (a) Fluorescence spectrum of UCNPs under 980 nm laser light excitation (red line) and UV/Vis absorption spectrum of SPCD (black line). (b) Formation of UCNPs coated with PS-doped dense silica. (c–e) Representative transmission electron micrographs of UCNPs, UCNP coated with dense silica, and UCNPs coated with dense and outer mesoporous silica shells (UC/PS). (f) Flow cytometric analyses of cell apoptosis treated with PBS, TPZ, UC/PS, or TPZ-UC/PS. Non-NIR: unirradiated cells; NIR: cells irradiated with 980 nm laser light.[69]

T, as TPZ remains active even under oxygen depletion conditions and induces cytotoxicity. This shows that chemo-T with TPZ can overcome the drawbacks of PDT in synergetic cancer treatment.

2.3 Covalent conjugation of PSs with UCNPs for PDT

The loading PS onto a porous silica shell or polymers coating on UCNPs *via* physical adsorption or physical encapsulation is simple and has a relatively high loading capacity. However, the downside is the highly limited FRET efficiency, as the SiO_2 shell raises the interval between UCNPs and PS.[69] Also, an unstable combination may cause PSs to pre-release before they reach the tumor, thereby further decreasing the effectiveness of the PDT. A suitable strategy to overcome the above-mentioned drawbacks might be to conjugate PS molecules onto the UCNP surface.[41] The photosensitization unit (CAOOH) is typically attached *via* an amide condensation reaction to the surface of UCNPs functionally linked with amino groups (ANH_2).[37] Liu *et al.* reported a covalent binding strategy to link rose bengal (FRET) to UCNPs, which had a high output level of $^1O_2$ (Fig. 7). They attempted to improve the FRET effectiveness to achieve a high quantum value of $^1O_2$.[70]

Xia *et al.* constructed a nanodevice named UCNPs-ZnPc, a highly efficient nanophotosensitizer for PDT, based on NIR light UCNPs and Zn(II)-phthalocyanine (ZnPc) PS.[71] The high $^1O_2$ production efficiency was achieved by enhancing the 660 nm upconversion emission of UCNPs through Yb^{3+} doping. The

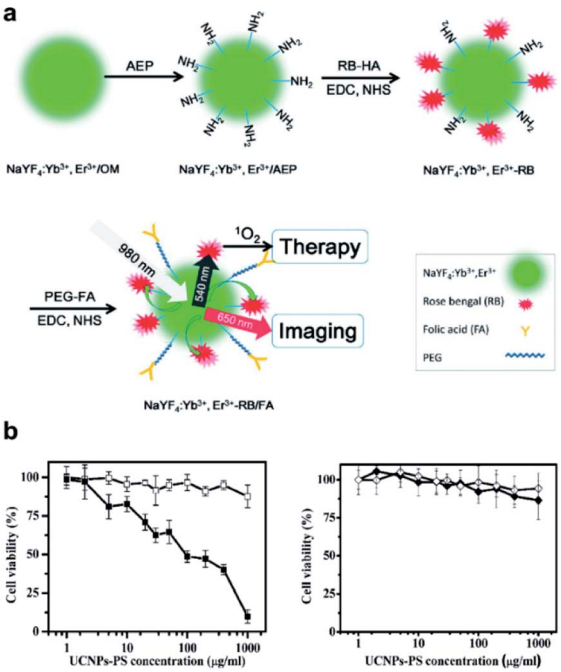

Fig. 7 (a) Schematic of covalent conjugation of $NaYF_4$:Yb^{3+}, Er^{3+} UCNPs, photosensitizer RB, and target molecule FA. (b) Viability of JAR cells (left) and NIH 3T3 fibroblasts (right) treated with UCNPs-PS of different concentrations with (solid) or without (open) 980 nm exposure.[70]

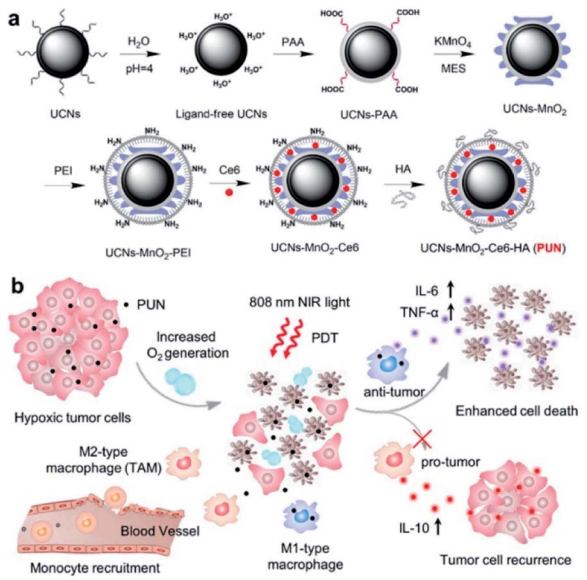

Fig. 8 Illustration of NIR light-mediated PDT strategy for the enhanced cellular ablation in tumor microenvironment. (a) Design and synthesis of PUN. (b) Scheme of improved therapy by attenuating hypoxia status and reprogramming TAMs from M2 to M1 phenotype to inhibit the recurrence of tumor cells toward immunotherapy during the post-PDT period.[72]

covalent linkage of UCNPs to ZnPc decreased the distance between the two and enhanced energy transfer. The high production of $^1O_2$, as shown in *in vivo* tests in which the material was injected locally into the tumor site of mice, could achieve safe and effective PDT treatment. The healthy organs showed no pathological and inflammatory changes. The deficiency of the design is the requirement of intratumoral injection, which is not suitable for deep tumors and not a safe way of determining changes of normal organs.

In order to increase the efficacy of an NIR-light-activated PDT by attenuating the status of tumor hypoxia and synergistically reprogramming the populations of tumor-related macrophages, Ai *et al.* constructed a unique PUN nanodevice (UCNs-MnO_2-Ce6-HA), with Ce6 loaded onto UCNPs, which was modified with manganese dioxide (MnO_2) nanosheets and then coated with hyaluronic acid (HA) biopolymer (Fig. 8). The system was able to react with overproduced H_2O_2, which is degraded by the MnO_2 nanosheets to produce a massive oxygen burst, and thus could significantly enhance PDT efficiency by 808 nm light irradiation. Furthermore, the bioinspired polymer HA could effectively reprogram the polarization of pro-tumor M2-type TAMs into anti-tumor M1-type macrophages to prevent tumor recurrence following PDT. Such promising results provided great opportunities for improved tumor ablation with NIR light-mediated PDT treatment by microtube attenuation and reprograming of tumor-related macrophages.[72]

Han's group designed a nanostructure using Nd^{3+} and Yb^{3+} as photosensitizers and Ho^{3+} as an active material.[73] Since Ho^{3+} emits light in the wavelength range of 540 nm and 650 nm in which rose bengal (RB) can be activated, it was used as a photosensitizer (Fig. 9). Covalent conjugation of the UCNPs with RB (UCNPs-RB) was designed in this study. By treating cells with UCNPs-RB followed by 808 nm light irradiation, a minimum overheating effect was verified by comparing UCNPs-RB treated cells with 980 nm light irradiation and the improved PDT efficiency was confirmed in HeLa cells.

Recently, Shi *et al.* designed a near infrared-driven PDT platform based on photosynthetic cyanobacterial cells hybridized with photosensitizer RB-loaded UCNPs, named UR-Cyan cells. Upon 980 nm NIR light irradiation, UR-Cyan cells showed strong oxygen production and further enhanced subsequent singlet oxygen generation by the photosensitizer, resulting in enhanced and sustainable PDT efficacy against tumor cells/tissues.[74] Compared to cell membranes and other cytoplasmic organelles, the nucleus is highly susceptible to photodynamic damage due to its high sensitivity to PDT.[75] Nucleus-based PDT can cause severe DNA damage and inactivation of intranuclear enzymes. Cell nucleus-based photodynamic therapy is a highly effective method for cancer treatment, but it is still challenging to design nucleus-targeting photosensitizers. Zhang *et al.* proposed a "one treatment, multiple irradiations" strategy to achieve nucleus-based photodynamic therapy based on RB-loaded MSN-coated UCNPs with amino-groups on the surface (UCNP/RB@mSiO_2-NH_2 NPs).[76] UCNP/RB@mSiO_2-NH_2 NPs could be specifically accumulated in the acidic lysosomes due to their amino group-decorated surface and the ROS produced by RB could effectively destroy lysosomes after 980 nm NIR light irradiation. Subsequently, UCNP/RB@mSiO_2-NH_2 NPs were released from the lysosomes and

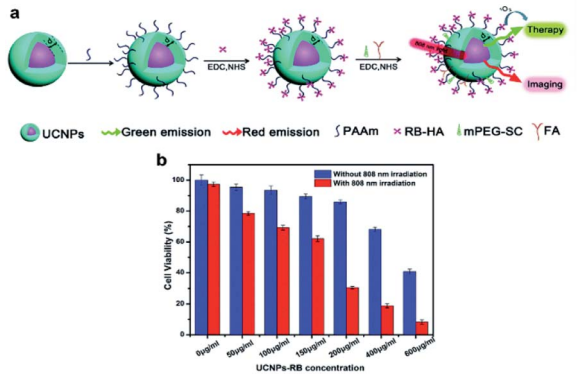

Fig. 9 (a) Schematic illustration of the synthetic step of 808 nm-activable UCNPs with RB. (b) Viability of HeLa cancer cells treated with different concentrations of UCNPs-RB with and without 808 nm laser irradiation (0.67 W cm^{-2}).[73]

were transferred into the cell nucleus, where a second round of 980 nm light irradiation achieved nucleus-based photodynamic therapy (Fig. 10).

We summarized the UCNP based PDT triggered by NIR light in Table 1. Despite its stable binding ability, the UCNP based PDT effect was still unsatisfactory, and this was mainly due to its relatively low conversion efficiency and weak PS loading, which further limits its application in *in vivo* anti-tumor studies.

3. Upconversion-based immunotherapy

Cancer immunotherapy has become a paradigm-shifting therapeutic approach, and various strategies have been developed in recent years, such as cancer vaccines,[90–92] chimeric antigen receptor (CAR)-T cell therapy,[93–96] immune checkpoint blockade (ICB) therapy,[97–100] cytokine therapy,[101–103] and immune adjuvant therapy,[104–106] showing striking clinical efficacy against tumors.[107–109] However, intravenous injection of immunotherapeutic agent is frequently accompanied by extreme side effects that seriously restrict the effectiveness of the remedy.[110,111] For example, the non-specific effects of immunotherapy agents on normal tissues, such as excessive cytokine release,[110] can lead to life-threatening complications (off-tumor toxicity). The risk of extreme toxicity is primarily due to a lack of accurate regulation of immunostimulatory activity

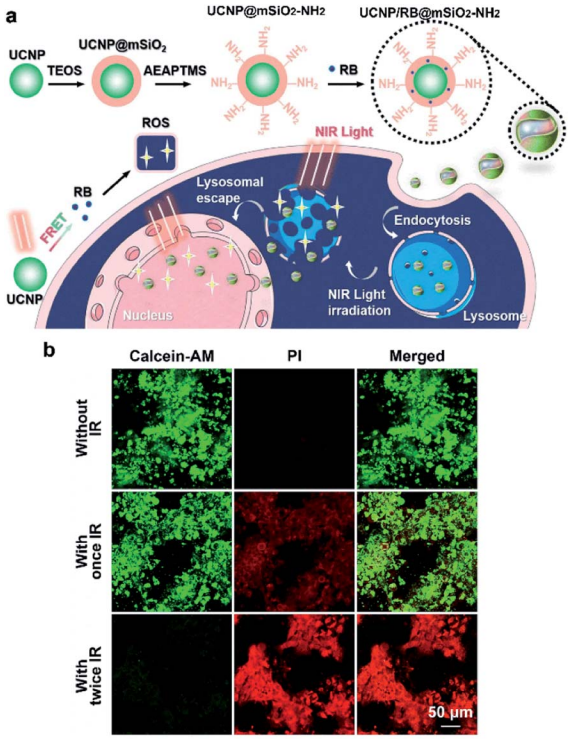

Fig. 10 (a) Schematic illustrations of the preparation of UCNP/RB@$mSiO_2$-NH_2 NPs and their application in the nucleus-based PDT of cancer cells based on the "one treatment, multiple irradiations" strategy. (b) CLSM images of MCF-7 cells treated as indicated and then double-stained with calcein AM and propidium iodide (PI). Scale bars, 50 μm.[76]

Table 1 Representative examples of UCNP-based PDT triggered by NIR light

PSs	Composite nanostructures	NIR laser (nm)	Laser dose (W cm^{-2})	Ref.
Ce6	UCNPs-Ce6	980	0.5	7
	UCNPs-Ce6	980	0.3	77
	UCNPs-Ce6-siRNA	980	0.8	78
	UCNP-Ce6-sgc8	980	0.6	79
	UCNP@2 × Ce6-DMMA-PEG	980	0.5	80
Porphyrin	UCNP-PEG-FA/PC70	980	0.8	81
	UCNP-TMPyP4-G4-aptamer	980	0.5	82
	UCNP-PJ	980	1.0	83
RB	UCNPs@RB@RGDRBC@ICG	980	1.5	84
	UCNPs-RB	808	1.15	85
	MUCNPs-800CW/Cy3/RB/Pep-QSY7	808	1.5	86
MOF	MOF-UCNP	980	15.9	87
	UCMTs	808	1.0	88
	CR@MUP	808	1.0	89

after the drug is injected into patients, and current approaches cannot effectively prevent systemic toxicity. Strategies aimed at precise exogenous modulation of the position and length of immune responses remain a key theme in cancer immunotherapy.[112,113] Nevertheless, it remains challenging to build regulatory frameworks to monitor antitumor immunity with great spatiotemporal precision. Due to their specific characteristics, UCNPs provide a strategy to control the delivery, release and activation of drugs. Consequently, UCNPs have been widely investigated in cancer immunotherapy in recent years.[114]

Xiang *et al.* were the first to develop antigen-loaded UCNPs for DC-based immunotherapy, and the system could be used to track dendritic cells *in vivo* using upconversion luminescence imaging.[115] Our team has developed an UCNPs-based immunotherapy device that enables remote control of antitumor immunity with NIR light both *in vitro* and *in vivo*. As shown in (Fig. 11), the immunotherapy device was constructed using

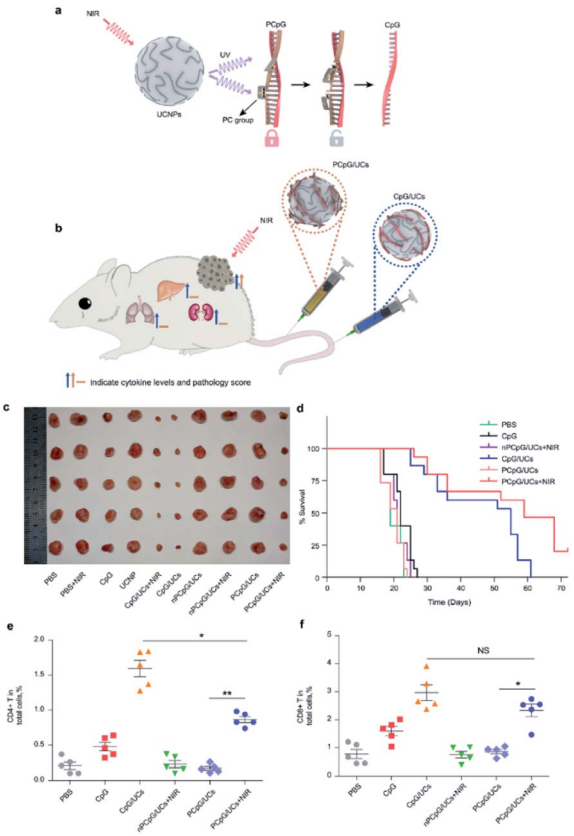

Fig. 11 (a) Schematic of the design of photoactivatable immunodevice through the integration of UCNPs with the UV light-responsive PCpG. UCNPs upconvert NIR light into UV light locally, thus liberate CpG ODN from PCpG to achieve immunotherapy effects; (b) illustration of the photoactivatable immunodevice, PCpG/UCs, for spatially selective triggering of immunoactivity through NIR light irradiation. In contrast to traditional CpG delivery system (CpG/UCs), PCpG/UCs is amenable to personalizing the antitumor modality with reduced systemic toxicity; (c) representative pictures of the tumors; (d) Kaplan–Meier survival curves of mice in the different treatment groups; (e and f) flow cytometric analysis of T cell populations in tumors from different treatment groups, showing percentages of total live cells.[116]

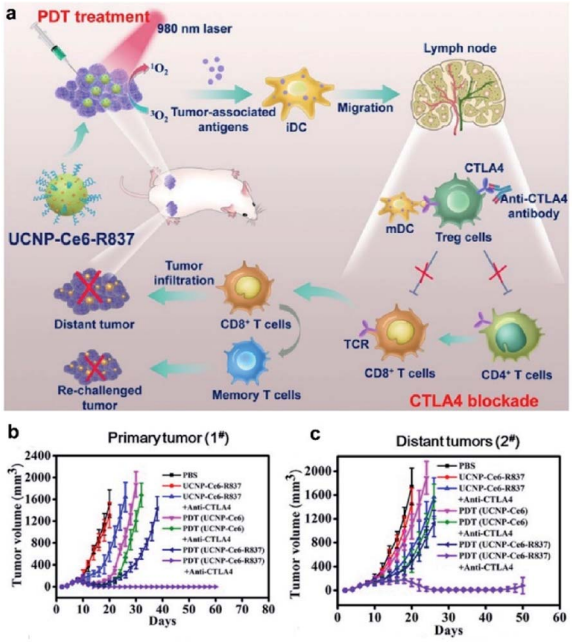

Fig. 12 (a) Schematic illustration of NIR triggered PDT with multitasking UCNPs in combination with checkpoint blockade for immunotherapy of cancer. (b) Growth curves for primary tumors (b) and distant tumors (c) on mice after various treatments indicated.[124]

UCNPs, immunotherapeutic CpG oligonucleotides and CpG complementary ssDNA containing photocleavable (PC) bonds that can be cleaved by UV light transduced by UCNPs, thus achieved remotely controlled immune triggering at the right time. The average size of the UC/PCpG is about 45 nm, which promotes the EPR effect.[116] However, one deficiency of this study is that the material reaches the tumor site through passive targeting, which is less effective than active targeting.

In recent years, a number of studies concentrated on immunotherapy combined with other treatments for cancer therapy.[117] In addition to being used as individual therapy, research has shed light on several potential alternative therapies, such as combining the sensitization effects of radiotherapy, chemotherapy, photothermal therapy (PTT), and immunotherapy, which show additive or synergistic benefits. PDT is an anticancer therapy that can induce immunogenic cell death and activate an adaptive immune response against tumor-associated antigens.[118–120] Many studies investigated synergistic treatments based on PDT and immunotherapy to trigger antitumor immunity.[121–123] Xu *et al.* conjugated the photosensitizer Ce6 and the Toll-like receptor 7 agonist R837 to UCNPs, obtaining multitasking UCNP-Ce6-R837 nanoparticles that could achieve effective PDT under NIR irradiation (Fig. 12). As expected, PDT triggered the release of tumor-associated antigens, while the R837-activated TLR7 pathway could induce strong systemic immunological responses and could be further enhanced by CTLA-4 blockade.[124] The greatest benefit of the system is that the nanodevice could prevent tumor recurrence *via* the immune memory effect.

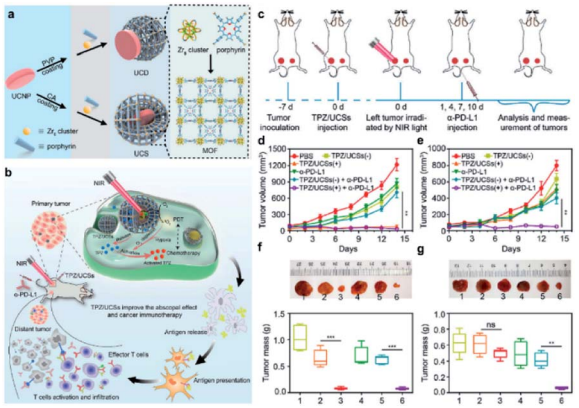

Fig. 13 (a) Schematic illustration of the synthesis of UCDs and UCSs through the conditional surface engineering of UCNPs. (b) Schematic illustration of the structure of TPZ/UCSs and their application for tumor treatment through the combination of NIR light-triggered PDT and hypoxia-activated chemotherapy with immunotherapy. (c) Schematic illustration of NIR light-triggered combinational therapy. Growth curves of (d) primary tumors and (e) distant tumors in CT26 tumor-bearing mice after different treatments. (f and g) Photos and average weights of primary tumors (left column) and distant tumors (right column) collected from mice 14 days after treatments.[125]

The combination of different therapy methods has become a smart strategy for cancer treatment. Recently, Li's group designed a composite nanomaterial that combined PDT, chemotherapy and immunotherapy together to fight hypoxic tumors.[125] They combined metal–organic frameworks (MOFs) and UCNPs to construct a heterostructure, which was then loaded with the hypoxia-activated prodrug tirapazamine (TPZ), thus combining NIR light-triggered PDT and chemotherapy against hypoxia tumors. Moreover, the integration of the composite nanoparticles with anti-programmed death ligand-1 (α-PD-L1) treatment completely inhibited distant tumors by inducing infiltration by cytotoxic T cells (Fig. 13).

Even though PDT and chemotherapy show clinical promise in destroying orthotopic tumors, they still show insufficient abscopal effects against metastases. The combination of PDT, chemotherapy and immunotherapy promises to exert a strong effect against distant metastases. Du *et al.* reported a new nanosystem that combines an anti-CD73 antibody and chemo-PDT to synergistically amplify the abscopal effects of T cell-mediated antitumor immunity.[126] The cancer cell membrane (CM)-cloaked UCNPs were integrated with RB and the ROS-sensitive polymer polyethylene glycol-thioketal-doxorubicin (PEG-TK-DOX), followed by their application for NIR-triggered chemo-PDT. The CM coating promoted the active targeting of the nanoparticles to the tumor and aided immune escape from macrophages. Chemo-PDT presents strong synergistic anti-tumor efficacy and causes immunogenic cell death (ICD), leading to tumor-specific immunity. The anti-CD73 antibody prevents immunosuppression by tumors and acts as a sufficient immune checkpoint blockade when combined with ICD-elicited tumor therapies (Fig. 14). Combined therapy, especially treatment approaches that incorporate immunotherapy, is a promising strategy for curing metastatic cancer in preclinical research. Chen *et al.* designed a UCNP-based antigen-capturing nanoplatform to synergize phototherapies and immunotherapy.[127] The nanoplatform is constructed *via* self-assembly of DSPE-PEG-maleimide and indocyanine green (ICG) onto UCNPs, followed by loading with the photosensitizer RB. ICG significantly enhances the efficiency of RB-based PDT upon NIR light activation, simultaneously achieving selective PTT. Most importantly, maleimide could capture and keep tumor associated antigens *in situ*, which were derived from phototherapy-treated tumor cells, and further enhance the uptake and presentation of tumor antigens. The combined PDT, PTT, and immunological effects induces a tumor-specific immune response. When combined with anti-CTLA-4, the nanoplatform showed a strong ability to destroy primary tumors and inhibit untreated distant tumors. Overall, combined immunotherapy provides a promising approach for the treatment of metastatic cancers.[128]

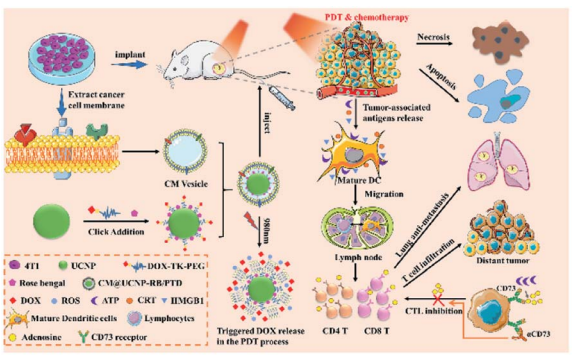

Fig. 14 Schematic illustration of the synthesis process of cancer membranes-camouflaged RB, DOX co-loaded UCNPs (CM@UCNP-RB/PTD) and the application in chemo-PDT combination therapy with CD73 blockade to enhance synergistic antitumor immunity in combating metastatic tumor.[126]

4. Upconversion-based gene therapy

Gene therapy holds great promise for the treatment of inherited diseases and cancer by targeted cells with therapeutic nucleic acids in order to repair abnormal gene expression.[129] Recently,

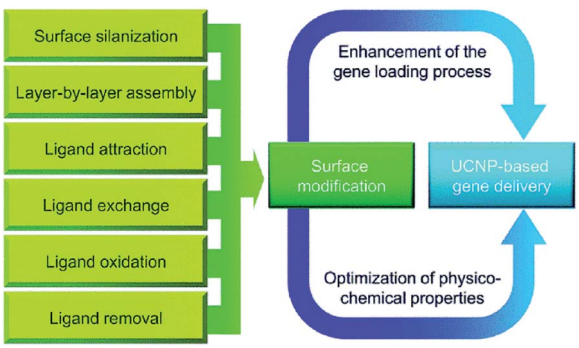

Fig. 15 Surface modification of UCNPs for gene delivery.[133]

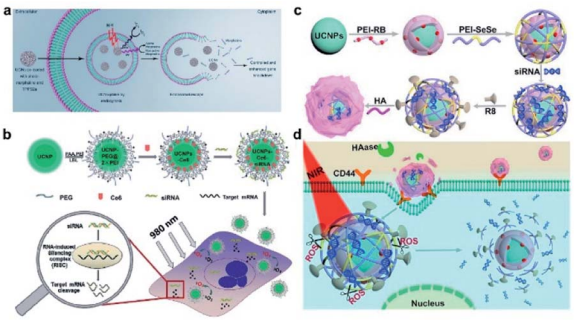

Fig. 16 Scheme representations of gene therapy with DNA-functionalized UCNPs. (a) Gene knockdown with UCNP-based photoactive delivery platform.[141] (b) The functionalization of UCNPs, co-loading with Ce6 and siRNA, and then the combined PDT and gene therapy delivered by UCNPs.[78] (c) Synthesis of UCNOs (UCNP-PEIRB-PEISeSe/siRNA-R8-HA), and (d) sequential responsive decompose of UCNOs and NIR boosted intracellular siRNA release and therapy.[144]

gene delivery has encountered bottlenecks in terms of performance and flexibility.[130] Since the beginning of this century, the controlled synthesis of uniform UCNPs has become mature and the research focus has shifted towards exploring biomedical applications of UCNPs.[131,132] Because of their unique characteristics as a modern method for increasing the flexibility of gene therapy, UCNPs have started to attract significant attention in recent years. Surface modifications can be made to improve UCNP-based gene carriers to achieve biological efficiency (Fig. 15).[133] The surface modification has two advantages. The first is to increase gene loading efficiency and the second is to optimize nanoparticles' physicochemical qualities for better biological performance.

A pioneering investigation of UCNPs for nucleic acids delivery was conducted by Zhang's group.[134] In their study, an anti-Her2 antibody was conjugated to amino-modified UCNPs for targeted delivery, and siRNAs were attached to the surface of UCNP-antiHer2 through electrostatic interactions. Material uptake by Her2-overexpressing SK-BR-3 cells was successfully confirmed, shown by the downregulated expression of the luciferase reporter gene. Subsequently, surface improvements to the abovementioned delivery system were further applied to improve the gene loading efficiency and increase the targeted distribution.[135–137] Recently, it was also demonstrated that UCNPs can be used to precisely regulate gene expression in tumor cells transplanted into adult zebrafish.[138] Similar success was also achieved using the NIR-to-UV upconversion process of silica-coated $NaYF_4$:Yb,Tm nanocrystals to temporally and spatially silence the expression of target genes.[139] This ability to manipulate gene expression has not only practical significance for the development of therapies, but also for basic research on signal transduction. All of these applications are beyond the scope of conventional gene delivery methods.

When a foreign gene is delivered into cells by the carrier, one important obstacle is that the sequestration of endosomal vesicles may lead to material degradation or exocytotic transport out of the cells.[140] Zhang's group used the photochemical internalization (PCI) method to enhance the endosomal escape of the delivered genes and boost the therapeutic effect. In said study, UCNPs were co-loaded with TPPS2a (PSs) and photo-morpholino (anti-STAT3, nucleic analogous for gene knockdown).[141] Under NIR excitation, TPPS2a was triggered by UCNP to generate ROS to locally disrupt the endosomal vesicle walls and trigger the release of the particles. At the same time, the UV light emitted by UCNPs cleaved the photo-morpholino senses strand and released the antisense morpholino, which further knocked down STAT3 gene expression (Fig. 16a). Compared to the control group, effective gene knockdown was achieved without facilitating endosomal escape demonstrating the excellent clinical application potential of this platform.

RNA interference (RNAi) is considered a promising tool for cancer treatment.[142] The high efficacy of siRNA is currently constrained by limitations of its delivery methods. Hence, improvements to the specificity and effectiveness of existing delivery systems are required before exploring clinical applications. Wang *et al.* engineered and synthesized polymer-coated UCNPs loaded with Ce6 and Plk1 oncogene-targeting siRNA

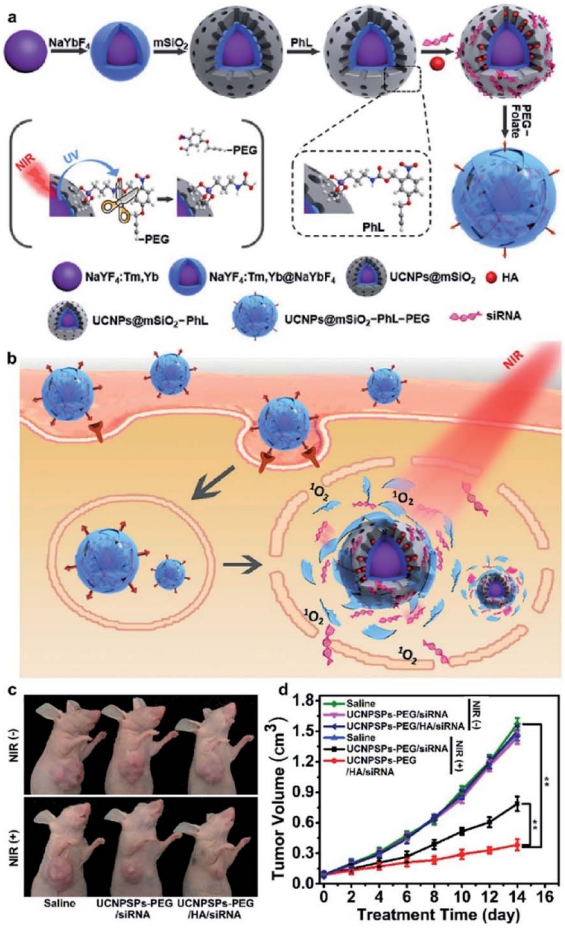

Fig. 17 Schematic illustrations of (a) synthesis of UCNP nanocapsules, and (b) folate receptor-mediated cellular uptake and NIR modulated intracellular siRNA delivery and therapy. (c) Demonstration of therapeutic efficiency with representative photos of xenograft tumors in mice on day 14 and (d) change of tumor volume as a function of time after treatment with the indicated materials.[145]

(Fig. 16b). The NIR laser-mediated PDT and siRNA delivery induced significant cancer cell apoptosis.[78] Such a combination of PDT and gene therapy greatly enhances the cancer cell killing effects and has relatively few side effects compared to conventional multimodal therapeutic systems focused on chemotherapy.

A key challenge in siRNA delivery is how to prevent the biomolecules from being degraded by enzymes in complicated physiological environments and how to trigger efficient on-demand release.[143] To solve this problem, He *et al.* designed a composite nanomaterial which is composed of UCNPs coated with PEI conjugated RB, and further coated with $^1O_2$ sensitive diselenide linked PEI, which was modified with therapeutic siRNA loading and cell-penetrating peptide R8, as well as an outer layer coated with hyaluronic acid (HA) (Fig. 16c).[144] NIR irradiation increased the decomposition of composite nanomaterials and induced the rapid and efficient release of siRNA, which effectively increased the *in vitro* gene silencing efficiency and *in vivo* tumor suppression (Fig. 16d). The sequentially sensitive UCNPs may have promising potential applications in precision medicine.

Recently, Zhang *et al.* developed a photo-degradable nano-capsule for efficient NIR-modulated siRNA delivery. The photo-degradable nano-capsules are based on core–shell UCNPs coated with an MSN layer for loading of photosensitizer HA and siRNA against polo-like kinase 1 (PLK1), covalently bound with a thin membrane of polyethylene glycol (PEG) *via* a synthesized photocleavable linker (PhL).[145] Upon 980 nm irradiation, the UCNPs produce UV emissions to break the PhL and detach the PEG membrane to release siRNA (Fig. 17a). ROS allows the cargo to escape the endosomes and increases the gene silencing performance, suppressing cell proliferation *in vitro* and tumor growth *in vivo* (Fig. 17b). The photo-degradable membrane-bound nano-capsules may have promising applications in precision medicine.

Lin *et al.* designed layer by layer UCNPs for monitoring and delivery of MDR1 gene-silencing siRNA (MDR1-siRNA) to enhance the effectiveness of chemotherapy by silencing the MDR1 gene and increase the drug sensitivity of ovarian cancer cells.[146] PAA and PEI were coated onto the surface of UCNOs and then loaded MDR1-siRNA by electrostatic adsorption (Fig. 18). The UCNP-based carrier increased the cellular uptake of MDR1-siRNA, protected them against nuclease-mediated degradation, and facilitated endosomal escape for effective MDR gene silencing.

5. Upconversion-based chemotherapy

Chemotherapy is the dominant treatment modality in modern cancer therapy, using chemical drugs to kill cancer cells. It typically works by preventing cancer cell growth, division and the creation of more cells.[147,148] Since cancer cells grow and divide faster than normal cells, chemotherapy has a much greater effect on cancer cells. However, due to low selectivity and high toxicity, the drugs used for chemotherapy exhibit

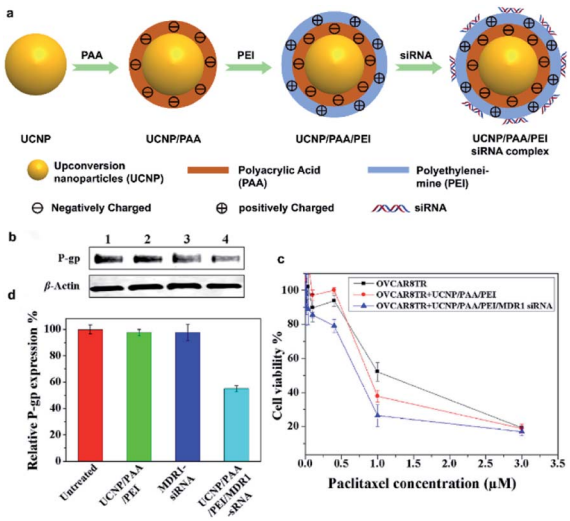

Fig. 18 (a) Schematic illustration for the preparation of layer-by-layer assembled UCNP/PAA/PEI/siRNA complex. (b) Western blot for the detection of P-gp expression in response to OVCAR8TR cells with different treatments. Lanes 1–4: untreated, UCNP/PAA/PEI, free MDR1-siRNA, and UCNP/PAA/PEI/MDR1-siRNA complex. (c) Quantitative analysis of P-gp expression. (d) OVCAR8TR cells viability to different treatments.[146]

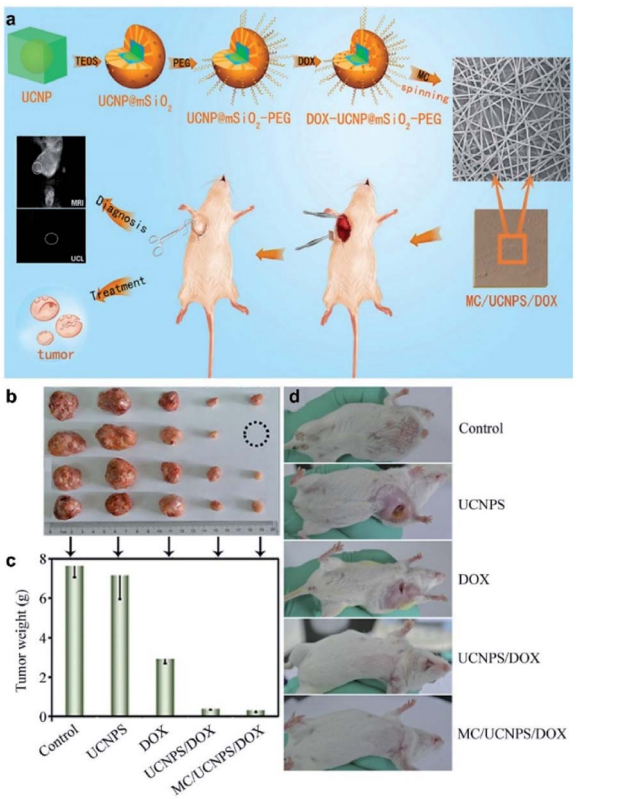

Fig. 19 (a) Schematic illustration for multifunctional MC/UCNPS/DOX nanofibers for synchronous up-conversion luminescence/magnetic resonance (UCL/MR) imaging and therapy of tumor *in vivo*. (b–d) The anti-tumor effects of the nanofibers *in vivo*.[157]

severe side-effects.[149–152] Enhancing selectivity is a crucial goal for increasing the therapeutic effectiveness of chemotherapy. Management of tumor chemotherapy to reduce systemic toxicity/adverse effects therefore has a pivotal significance.[152–154]

Due to their capacity to specifically bind to targets and deliver a large amount of therapeutic drugs, nanoparticles have attracted wide attention in medicine. Such materials could be adapted for cancer chemotherapy and various other diseases by making therapeutic delivery into diseased cells more efficient while lowering the exposure of healthy tissue to toxic side effects.[155,156] Accordingly, UCNPs have been studied as nanocarriers for anticancer drugs using appropriate surface modification and functionalization. However, pre-release of anticancer drugs before the particles arrived at the target might lead to severe side effects and reduce their effectiveness. To solve this problem, there is a great need to develop UCNP-based targeted drug delivery systems, which can be used as contrast agents for bioimaging and on-demand drug release. However, few UCNP-based single chemotherapy studies were reported, and most studies were focused on the combination of UCNP-based chemotherapy with other therapies, such as PDT or photothermal therapy (PTT).

Chen *et al.* developed a multifunctional, dual-drug carrier platform based on UCNPs@SiO_2 loaded doxorubicin (DOX), poly(ε-caprolactone) and gelatin loaded with an anti-inflammatory drug together with indomethacin to form nanofibrous fabrics.[157] These nanofibrous fabrics can be implanted at the tumor site to exert orthotopic chemotherapy by controlled release of DOX from mesoporous SiO_2 (Fig. 19a). This nanoplatform showed an excellent antitumor effect *in situ* (Fig. 19b–d), and the nanofibers can also be used for fluorescence/magnetic resonance dual-model imaging (Fig. 19a).

In addition to direct delivery of chemotherapy drugs to the tumor site, UCNPs can be designed to construct TME responsive drug release systems. Li *et al.* designed a pH-responsive nanoparticle WP5⊃1-UCNPs (Fig. 20a). Carboxylatebased pillar arene (WP5) and 15-carboxy-*N*,*N*,*N*-trialkylpentadecan-1-ammonium bromide (1)-functionalized UCNPs can be decomposed by the acidic lysosome to release DOX loaded onto the UCNPs@SiO_2.[158] Cytotoxicity experiments have shown the outstanding biocompatibility of WP5⊃1-UCNPs without DOX loading, and that the DOX-WP5⊃1-UCNPs nanosystem has been proved to effectively kill HeLa cells (Fig. 20b).

Relying on chemotherapy alone cannot always achieve the desired therapeutic effects. Almost all of the UCNP-based chemotherapy platforms were designed for combination with other therapies, such as PDT, PTT, immunotherapy and so on.[159–161] Stimuli-responsive nanoparticles with multiple therapeutic functions are highly attractive for effective tumor treatment.[162–166] Zhao *et al.* designed a composite nanoparticle named MPPa/UCNP-DEVD-DOX/cRGD, which was formulated by the assembly of UCNP, caspase-3 responsive DOX, a photosensitizer (pyropheophorbide-a methyl ester, MPPa) and tumor-targeting cRGD-PEG-DSPE to afford multifunctional CFUNs (Fig. 21a).[167] After the particles were delivered into the cells, NIR irradiation was applied and the UCNPs emitted visible light inducing MPPa to produce ROS for PDT. Caspase-3 then triggered the release of DOX within tumor cells, thus

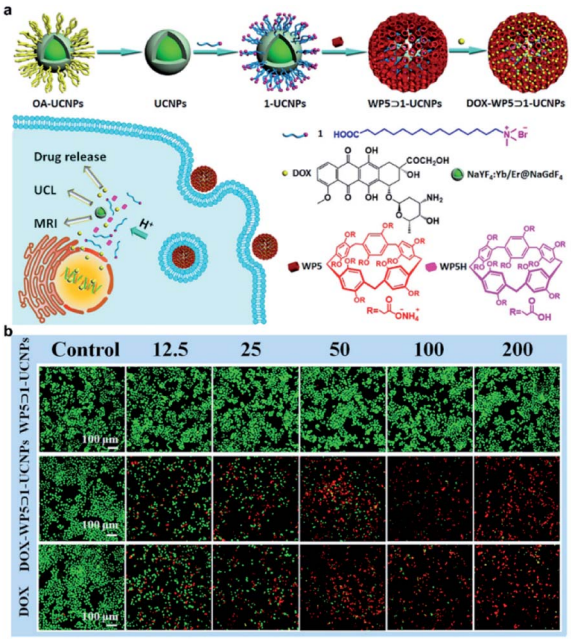

Fig. 20 (a) Schematic illustration of the synthesis of DOX-WP5⊃1-UCNPs and the UCNPs based TME responsive drug-releasing nanosystem. (b) Fluorescence microscopy images of calcein-AM/ethidium homodimer-1-stained HeLa cells (green represents living cells, red represents dead cells) incubated with the concentration range of 12.5–200 μg mL^{-1} of WP5⊃1-UCNPs or DOX-WP5⊃1-UCNPs, or DOX.[158]

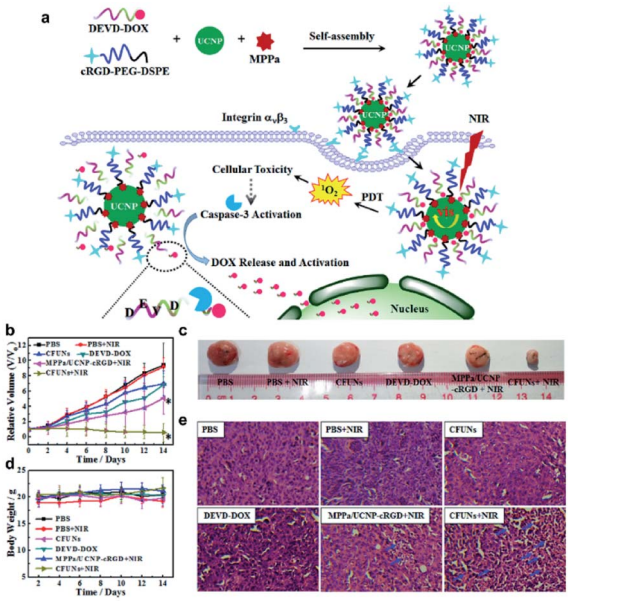

Fig. 21 (a) Schematic illustration of the synthesis of MPPa/UCNP-DEVD-DOX/cRGD and the mechanism of anti-tumor effect of the particles. (b) Relative volume of the tumor. (c) Representative pictures of the tumors. (d) Body weight of each mouse. (e) Histological assessments of tissues using H&E staining in the different treatment groups.[167]

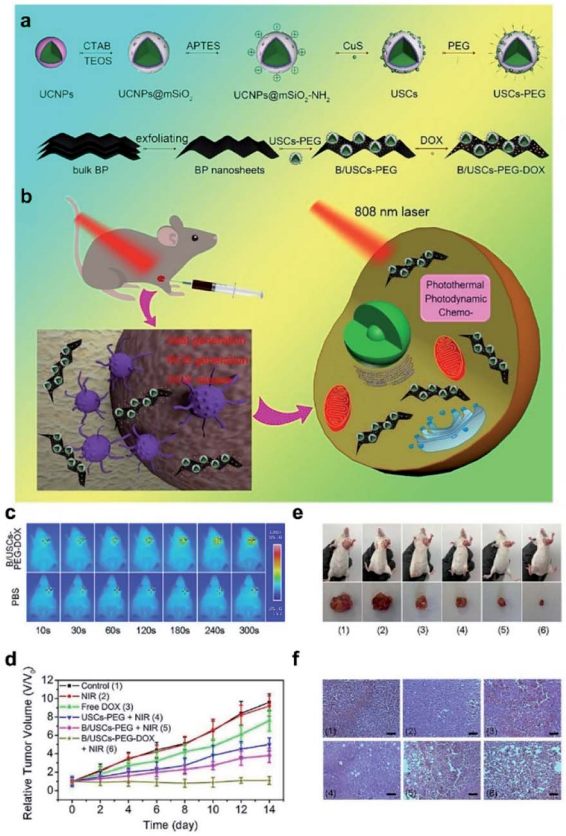

Fig. 22 (a) Schematic illustration of the synthesis of B/USCs-PEG-DOX and the release of loaded DOX. (b) The mechanism of anti-tumor effect of the particles. (c–f) The antitumor effects of the composite nanosystem.[168]

accomplishing NIR-triggered PDT and cascade chemotherapy. The CFUN system enables the spatiotemporal control of NIR-triggered cascade therapeutic activation and tumor inhibition due to consecutive PDT and chemotherapy (Fig. 21b–e).

Recently, Xu *et al.* designed a composite nanosystem through the incorporation of copper sulfide (CuS) nanosheets with strong negative charges into mesoporous silica UCNPs (Fig. 22a).[168] After DOX loading, synergistic treatment *via* PTT, PDT and chemotherapy can be accomplished. The nanocomposites demonstrated excellent anti-tumor efficacy under 808 nm light irradiation, overcoming the low efficiency and limited penetration depth of traditional UV light (Fig. 22b–f).

Despite remarkable progresses in nucleic acid-targeted tumor therapy, there are few reports on intracellular RNA and nuclear DNA-dual targeted cancer treatments *via* a single nanodelivery system.[169] Ma *et al.* designed an upconversion nanoplatform *cis*-platinum pro-drug (DSP) and cytotoxic protein ribonuclease A (RNase A) dual-therapeutic agent-loaded large-pore mesoporous silica-coated β-$NaYF_4$:20%Yb,2%Er@β-$NaGdF_4$ upconversion nanoplatform for chemo-protein combination therapy. The nanosystem can not only transport cytotoxic protein molecules and *cis*-platin pro-drugs into tumor cells to induce intracellular RNA degradation-mediated and nuclear DNA-targeted killing of cancer cells, but also achieve upconversion luminescence (UCL) and magnetic resonance (MR) dual-mode bioimaging (Fig. 23).[169] Moreover, the synergetic treatment *via* chemotherapy and protein therapy exhibits a better therapeutic effect *in vivo* compared with chemotherapy or protein therapy alone. This relatively simple RNA and DNA-dual-targeted nanosystem will open new avenues for cancer therapy.

Chemotherapy remains the gold standard for the treatment of non-resectable tumors, but there still remains the problem of the systematic toxicity of the drugs. Even though a lot of progress has been made, we still need to explore more sophisticated nanosystems to solve this pressing problem.

6. Toxic side-effects of upconversion-based therapy

Lanthanide-based UCNPs that convert NIR light into visible or ultraviolet light have many advantages, including deep tissue penetration, long-term fluorescence and less tissue-photodamage. These benefits make UCNPs an effective carrier for drugs and light-driven drug activation for cancer therapy.[170–172] Due to the increasing applications and interest in other areas in the biomedical field, UCNPs may be released into the environment, raising concerns about their possible environmental and human health hazards. In particular, UCNPs may exhibit *in vivo* toxicity related to their metabolization. The toxicological safety and metabolization of UCNP materials have therefore become a major concern.

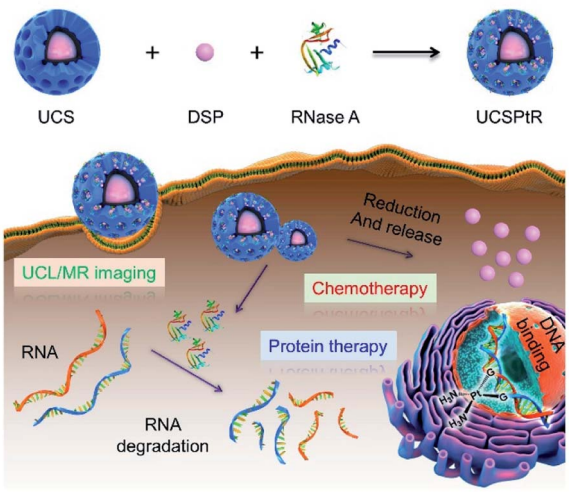

Fig. 23 Schematic illustration of UCSPtR for UCL/MR dual-mode bioimaging and chemo/protein combined therapy. Quadrivalent *cis*-platinum prodrugs, DSP and cytotoxic protein RNase A were loaded into large-pore mesoporous silica-coated β-$NaYF_4$:20%Yb,2%Er@β-$NaGdF_4$ (UCS) nanoparticles to obtain UCSPtR nanocomposites. Once internalized, this nanoplatform can effectively release cytotoxic protein and DSP and thus induce intracellular RNA degradation-mediated and nuclear DNA-targeted killings of cancer cells, respectively, to achieve collaborative treatments of chemotherapy and protein therapy. Furthermore, upconversion luminescence (UCL) and magnetic resonance (MR) dual-mode bioimaging can be achieved simultaneously.[169]

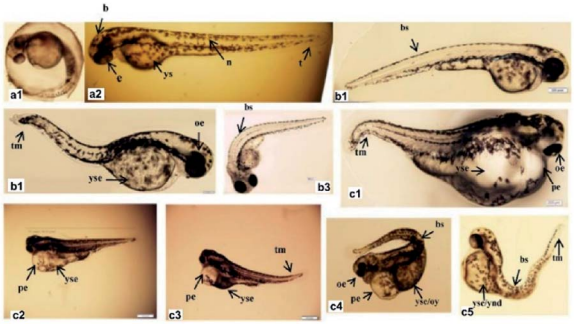

Fig. 24 Phenotypic changes of zebrafish embryos at 48 hpf. (a1, a2) Control group. (b1–b3) UCNPs <200 μg mL^{-1} groups. (c1–c5) UCNPs 200–400 μg mL^{-1} groups. Abbreviations: b, brain; e, eye; n, notochord; t, tail; ys, yolk sac; bs, bent spine; tm, tail malformation; oe, ocular edema; pe, pericardial edema; oy, opaque yolk; yes, yolk sac edema; and ynd, yolk not depleted.[174]

Yu *et al.* carried out a systematic study to compare the *in vivo* biodistribution, excretion, and biosafety of PEI modified $NaYF_4$:Yb,Er (PEI@UCNPs) among three different exposure routes (IV, IP, and IG).[173] A variety of methods, including inductive coupling plasma mass spectrometry (IPC-SM), histology, body weight and biochemical analysis were used to assess the biodistribution, excretion and biosafety of UCNPs, and no obvious toxicity of UCNPs was observed in mice exposed through either of the tested administration routes. Wang *et al.* designed an experiment to evaluate the effects of LaF_3:Yb,Er UCNPs on zebrafish embryos.[174] The results showed that LaF_3:Yb,Er UCNPs did not exhibit obvious toxicity to zebrafish embryos at a relative low dose (<100 mg L^{-1}) but exhibited chronic toxicity at relatively high does (>200 mg L^{-1}) *in vivo*, resulting in malformations and a reduced hatching rate, as well as impeding embryonic and larval development (Fig. 24). Xiong *et al.* explored the chronic toxicity of PAA modified UCNPs in mice exposed up to 115 days.[175] PAA-UCNPs did not exhibit overt toxicity to mice and the studies indicate that PAA-UNCPs may probably be used long-term for targeted imaging and therapeutic studies *in vivo*. We also investigated the toxicity of UCNPs to mice by tail vein injection.[25] The pathology of normal organs (heart, liver, spleen, lungs and kidneys) showed no change compared with the control group, and there were also no changes in the serum levels of cytokines, alanine aminotransferase (ALT) and aspartate aminotransferase (AST). The study indicated that UCNPs have low systematic toxicity and are suitable for *in vivo* applications. Although several studies have demonstrated the short-term safety of UCNPs *in vitro* or *in vivo*, their long-term chronic effects and bio accumulation potential are poorly understood.[176,177]

7. Summary and perspectives

In this review, we outlined recent developments in UCNP-based light-activated tumor therapy, including PDT, immunotherapy, gene therapy, chemo-therapy and combination therapy. As can be seen in the paper, significant progress has been made in UCNP-based cancer therapy. Despite these promising findings, there are several problems for nanomaterials that need to overcome to achieve the goal of nanomaterials-based cancer therapy.

(i) Rational combination of therapeutic modalities: the current development of UCNP-based nanocarriers aims to create a single dose magic bullet combined with different treatments for cancer therapy. It is therefore important to boost the therapeutic efficacy at a lower dose while promoting a biocompatible carrier material and to decrease toxic side effects. Although some combinations were successfully introduced and had good results as planned, UCNP-based combined cancer treatment is still in the early stages. In addition, the random combination of therapeutic strategies not only leads to challenges in achieving the above-noted goal of synergistic cancer therapy, but may also have unforeseen and unintended harmful consequences. In addition, the unique spatiotemporal form of each monotherapy should be considered to target cancer when combining monotherapies for synergistic therapy.

(ii) The key potential risks in the clinical application of UCNPs are their systemic toxicity, the complexity of clearance and long-term effects on the human body. Furthermore, the relationship between the immune system, its interference with the reproductive system and its effect on the next generation are still uncertain. More systematic studies are also required for safety assessment before these particles are used in the clinic.

Conflicts of interest

There are no conflicts to declare.

Acknowledgements

This work was supported financially by National Natural Science Foundation of China (82001946, 21805060), Beijing Municipal Natural Science Foundation (7214300) and Beijing Municipal Administration of Hospitals Incubating Program (PX2021061).

References

1 M. S. Copur, *Oncology*, 2019, **33**, 181–185.
2 H. Yuan, A. M. Fales and T. Vo-Dinh, *J. Am. Chem. Soc.*, 2012, **134**, 11358–11361.
3 M. Ding, J. Li, X. He, N. Song, H. Tan, Y. Zhang, L. Zhou, Q. Gu, H. Deng and Q. Fu, *Adv. Mater.*, 2012, **24**, 3639–3645.
4 S. S. Oh, B. F. Lee, F. A. Leibfarth, M. Eisenstein, M. J. Robb, N. A. Lynd, C. J. Hawker and H. T. Soh, *J. Am. Chem. Soc.*, 2014, **136**, 15010–15015.
5 M. Chanana, P. Rivera Gil, M. A. Correa Duarte, L. M. Liz Marzán and W. J. Parak, *Angew. Chem., Int. Ed.*, 2013, **52**, 4179–4183.
6 K. H. Bae, H. J. Chung and T. G. Park, *Mol. Cells*, 2011, **31**, 295–302.
7 C. Wang, H. Tao, L. Cheng and Z. Liu, *Biomaterials*, 2011, **32**, 6145–6154.

8 K. Ulbrich, K. Hola, V. Subr, A. Bakandritsos, J. Tucek and R. Zboril, *Chem. Rev.*, 2016, **116**, 5338–5431.
9 S. Baek, R. K. Singh, D. Khanal, K. D. Patel, E. Lee, K. W. Leong, W. Chrzanowski and H. Kim, *Nanoscale*, 2015, **7**, 14191–14216.
10 X. Lv, Y. Zhu, H. Ghandehari, A. Yu and Y. Wang, *Chem. Commun.*, 2019, **55**, 3383–3386.
11 A. O. Elzoghby, W. M. Samy and N. A. Elgindy, *J. Controlled Release*, 2012, **157**, 168–182.
12 S. Zhang, Z. Chu, C. Yin, C. Zhang, G. Lin and Q. Li, *J. Am. Chem. Soc.*, 2013, **135**, 5709–5716.
13 H. Xiao, G. T. Noble, J. F. Stefanick, R. Qi, T. Kiziltepe, X. Jing and B. Bilgicer, *J. Controlled Release*, 2014, **173**, 11–17.
14 A. Jana, K. T. Nguyen, X. Li, P. Zhu, N. S. Tan, H. Ågren and Y. Zhao, *ACS Nano*, 2014, **8**, 5939–5952.
15 S. Wen, J. Zhou, K. Zheng, A. Bednarkiewicz, X. Liu and D. Jin, *Nat. Commun.*, 2018, **9**, 1.
16 H. Mai, Y. Zhang, R. Si, Z. Yan, L. Sun, L. You and C. Yan, *J. Am. Chem. Soc.*, 2006, **128**, 6426–6436.
17 F. Auzel, *Chem. Rev.*, 2004, **104**, 139–173.
18 H. Dong, S. Du, X. Zheng, G. Lyu, L. Sun, L. Li, P. Zhang, C. Zhang and C. Yan, *Chem. Rev.*, 2015, **115**, 10725–10815.
19 J. Zhao, J. Gao, W. Xue, Z. Di, H. Xing, Y. Lu and L. Li, *J. Am. Chem. Soc.*, 2018, **140**, 578–581.
20 J. Zhao, H. Chu, Y. Zhao, Y. Lu and L. Li, *J. Am. Chem. Soc.*, 2019, **141**, 7056–7062.
21 M. Li, J. Zhao, H. Chu, Y. Mi, Z. Zhou, Z. Di, M. Zhao and L. Li, *Adv. Mater.*, 2019, **31**, 1804745.
22 N. Bogdan, F. Vetrone, G. A. Ozin and J. A. Capobianco, *Nano Lett.*, 2011, **11**, 835–840.
23 R. Deng, J. Wang, R. Chen, W. Huang and X. Liu, *J. Am. Chem. Soc.*, 2016, **138**, 15972–15979.
24 B. Gu and Q. Zhang, *Adv. Sci.*, 2018, **5**, 1700609.
25 H. Chu, J. Zhao, Y. Mi, Z. Di and L. Li, *Nat. Commun.*, 2019, **10**, 1.
26 D. E. Dolmans, D. Fukumura and R. K. Jain, *Nat. Rev. Cancer*, 2003, **3**, 380–387.
27 S. B. Brown, E. A. Brown and I. Walker, *Lancet Oncol.*, 2004, **5**, 497–508.
28 X. Shi, C. Y. Zhang, J. Gao and Z. Wang, *Wiley Interdiscip. Rev.: Nanomed. Nanobiotechnol.*, 2019, **11**, e1560.
29 J. W. Snyder, W. R. Greco, D. A. Bellnier, L. Vaughan and B. W. Henderson, *Cancer Res.*, 2003, **63**, 8126–8131.
30 Y. Liu, K. Ma, T. Jiao, R. Xing, G. Shen and X. Yan, *Sci. Rep.*, 2017, **7**, 42978.
31 M. B. Vrouenraets, G. W. Visser, G. B. Snow and G. A. Van Dongen, *Anticancer Res.*, 2003, **23**, 505–522.
32 Z. Luksiene, I. Eggen, J. Moan, J. M. Nesland and Q. Peng, *Cancer Lett.*, 2001, **169**, 33–39.
33 Y. Wang, Y. Lin, H. Zhang and J. Zhu, *J. Cancer Res. Clin. Oncol.*, 2016, **142**, 813–821.
34 Y. Zhang, L. He, J. Wu, K. Wang, J. Wang, W. Dai, A. Yuan, J. Wu and Y. Hu, *Biomaterials*, 2016, **107**, 23–32.
35 J. Xie, Y. Wang, W. Choi, P. Jangili, Y. Ge, Y. Xu, J. Kang, L. Liu, B. Zhang, Z. Xie, J. He, N. Xie, G. Nie, H. Zhang and J. S. Kim, *Chem. Soc. Rev.*, 2021, **50**, 9152–9201.
36 S. S. Lucky, K. C. Soo and Y. Zhang, *Chem. Rev.*, 2015, **115**, 1990–2042.
37 Y. Liu, X. Meng and W. Bu, *Coord. Chem. Rev.*, 2019, **379**, 82–98.
38 D. Yang, Z. Hou, Z. Cheng, C. Li and J. Lin, *Chem. Soc. Rev.*, 2015, **44**, 1416–1448.
39 D. K. Chatterjee and Z. Yong, *Nanomedinine*, 2008, **3**, 73–82.
40 C. Wang, L. Cheng and Z. Liu, *Biomaterials*, 2011, **32**, 1110–1120.
41 C. Wang, L. Cheng and Z. Liu, *Theranostics*, 2013, **3**, 317–330.
42 M. Manzano and M. Vallet Regí, *Adv. Funct. Mater.*, 2020, **30**, 1902634.
43 M. Vallet-Regi, A. Ramila, R. P. Del Real and J. Pérez-Pariente, *Chem. Mater.*, 2001, **13**, 308–311.
44 P. Yang, S. Gai and J. Lin, *Chem. Soc. Rev.*, 2012, **41**, 3679–3698.
45 S. Huh, J. W. Wiench, J. Yoo, M. Pruski and V. S. Lin, *Chem. Mater.*, 2003, **15**, 4247–4256.
46 B. G. Trewyn, C. M. Whitman and V. S. Lin, *Nano Lett.*, 2004, **4**, 2139–2143.
47 K. Suzuki, K. Ikari and H. Imai, *J. Am. Chem. Soc.*, 2004, **126**, 462–463.
48 J. Y. Ying, *Chem. Eng. Sci.*, 2006, **61**, 1540–1548.
49 J. Y. Ying, C. P. Mehnert and M. S. Wong, *Angew. Chem., Int. Ed.*, 1999, **38**, 56–77.
50 C. T. Kresge, M. E. Leonowicz, W. J. Roth, J. C. Vartuli and J. S. Beck, *Nature*, 1992, **359**, 710–712.
51 T. Xia, M. Kovochich, M. Liong, H. Meng, S. Kabehie, S. George, J. I. Zink and A. E. Nel, *ACS Nano*, 2009, **3**, 3273–3286.
52 H. Meng, M. Liong, T. Xia, Z. Li, Z. Ji, J. I. Zink and A. E. Nel, *ACS Nano*, 2010, **4**, 4539–4550.
53 H. Meng, M. Xue, T. Xia, Y. Zhao, F. Tamanoi, J. F. Stoddart, J. I. Zink and A. E. Nel, *J. Am. Chem. Soc.*, 2010, **132**, 12690–12697.
54 B. Munoz, A. Ramila, J. Perez-Pariente, I. Diaz and M. Vallet-Regi, *Chem. Mater.*, 2003, **15**, 500–503.
55 C. Hom, J. Lu, M. Liong, H. Luo, Z. Li, J. I. Zink and F. Tamanoi, *Small*, 2010, **6**, 1185.
56 C. Li, D. Yang, P. Ma, Y. Chen, Y. Wu, Z. Hou, Y. Dai, J. Zhao, C. Sui and J. Lin, *Small*, 2013, **9**, 4150–4159.
57 M. Lin, Y. Gao, F. Hornicek, F. Xu, T. J. Lu, M. Amiji and Z. Duan, *Adv. Colloid Interface Sci.*, 2015, **226**, 123–137.
58 P. Zhang, W. Steelant, M. Kumar and M. Scholfield, *J. Am. Chem. Soc.*, 2007, **129**, 4526–4527.
59 F. Chen, S. Zhang, W. Bu, Y. Chen, Q. Xiao, J. Liu, H. Xing, L. Zhou, W. Peng and J. Shi, *Chem.–Eur. J.*, 2012, **18**, 7082–7090.
60 N. M. Idris, M. K. Gnanasammandhan, J. Zhang, P. C. Ho, R. Mahendran and Y. Zhang, *Nature Medicine*, 2012, **18**, 1580–1585.
61 C. Wang, L. Cheng, Y. Liu, X. Wang, X. Ma, Z. Deng, Y. Li and Z. Liu, *Adv. Funct. Mater.*, 2013, **23**, 3077–3086.
62 Q. Yuan, Y. Wu, J. Wang, D. Lu, Z. Zhao, T. Liu, X. Zhang and W. Tan, *Angew. Chem., Int. Ed.*, 2013, **52**, 13965–13969.

63 L. Zeng, L. Xiang, W. Ren, J. Zheng, T. Li, B. Chen, J. Zhang, C. Mao, A. Li and A. Wu, *RSC Adv.*, 2013, **3**, 13915–13925.
64 R. Rafique, A. R. Gul, I. G. Lee, S. H. Baek, S. K. Kailasa, N. Iqbal, E. J. Cho, M. Lee and T. J. Park, *Mater. Sci. Eng., C*, 2020, **110**, 110545.
65 Y. Mi, H. Cheng, H. Chu, J. Zhao, M. Yu, Z. Gu, Y. Zhao and L. Li, *Chem. Sci.*, 2019, **10**, 10231–10239.
66 A. L. Harris, *Nat. Rev. Cancer*, 2002, **2**, 38–47.
67 J. M. Brown and W. R. Wilson, *Nat. Rev. Cancer*, 2004, **4**, 437–447.
68 W. R. Wilson and M. P. Hay, *Nat. Rev. Cancer*, 2011, **11**, 393–410.
69 Y. Liu, Y. Liu, W. Bu, C. Cheng, C. Zuo, Q. Xiao, Y. Sun, D. Ni, C. Zhang and J. Liu, *Angew. Chem., Int. Ed.*, 2015, **127**, 8223–8227.
70 K. Liu, X. Liu, Q. Zeng, Y. Zhang, L. Tu, T. Liu, X. Kong, Y. Wang, F. Cao and S. A. Lambrechts, *ACS Nano*, 2012, **6**, 4054–4062.
71 L. Xia, X. Kong, X. Liu, L. Tu, Y. Zhang, Y. Chang, K. Liu, D. Shen, H. Zhao and H. Zhang, *Biomaterials*, 2014, **35**, 4146–4156.
72 X. Ai, M. Hu, Z. Wang, L. Lyu, W. Zhang, J. Li, H. Yang, J. Lin and B. Xing, *Bioconjugate Chem.*, 2018, **29**, 928–938.
73 D. Wang, B. Xue, X. Kong, L. Tu, X. Liu, Y. Zhang, Y. Chang, Y. Luo, H. Zhao and H. Zhang, *Nanoscale*, 2015, **7**, 190–197.
74 M. Huo, P. Liu, L. Zhang, C. Wei, L. Wang, Y. Chen and J. Shi, *Adv. Funct. Mater.*, 2021, **31**, 2010196.
75 Y. Yang, W. Zhu, L. Feng, Y. Chao, X. Yi, Z. Dong, K. Yang, W. Tan, Z. Liu and M. Chen, *Nano Lett.*, 2018, **18**, 6867–6875.
76 X. Chen, Y. Zhang, X. Zhang, Z. Zhang and Y. Zhang, *Mikrochim. Acta*, 2021, **188**, 349.
77 Y. I. Park, H. M. Kim, J. H. Kim, K. C. Moon, B. Yoo, K. T. Lee, N. Lee, Y. Choi, W. Park and D. Ling, *Adv. Mater.*, 2012, **24**, 5755–5761.
78 X. Wang, K. Liu, G. Yang, L. Cheng, L. He, Y. Liu, Y. Li, L. Guo and Z. Liu, *Nanoscale*, 2014, **6**, 9198–9205.
79 W. Hou, Y. Liu, Y. Jiang, Y. Wu, C. Cui, Y. Wang, L. Zhang, I. Teng and W. Tan, *Nanoscale*, 2018, **10**, 10986–10990.
80 C. Wang, L. Cheng, Y. Liu, X. Wang, X. Ma, Z. Deng, Y. Li and Z. Liu, *Adv. Funct. Mater.*, 2013, **23**, 3077–3086.
81 M. Guan, H. Dong, J. Ge, D. Chen, L. Sun, S. Li, C. Wang, C. Yan, P. Wang and C. Shu, *NPG Asia Mater.*, 2015, **7**, e205.
82 Q. Yuan, Y. Wu, J. Wang, D. Lu, Z. Zhao, T. Liu, X. Zhang and W. Tan, *Angew. Chem., Int. Ed.*, 2013, **52**, 13965–13969.
83 X. Sun, P. Zhang, Y. Hou, Y. Li, X. Huang, Z. Wang, L. Jing and M. Gao, *Chem. Eng. Process.*, 2019, **142**, 107551.
84 P. Wang, X. Wang, Q. Luo, Y. Li, X. Lin, L. Fan, Y. Zhang, J. Liu and X. Liu, *Theranostics*, 2019, **9**, 369.
85 D. Wang, B. Xue, X. Kong, L. Tu, X. Liu, Y. Zhang, Y. Chang, Y. Luo, H. Zhao and H. Zhang, *Nanoscale*, 2015, **7**, 190–197.
86 Y. Li, X. Zhang, Y. Zhang, Y. Zhang, Y. He, Y. Liu and H. Ju, *ACS Appl. Mater. Interfaces*, 2020, **12**, 19313–19323.
87 L. He, M. Brasino, C. Mao, S. Cho, W. Park, A. P. Goodwin and J. N. Cha, *Small*, 2017, **13**, 1700504.
88 C. Liu, B. Liu, J. Zhao, Z. Di, D. Chen, Z. Gu, L. Li and Y. Zhao, *Angew. Chem., Int. Ed.*, 2020, **59**, 2634–2638.
89 Z. Li, X. Qiao, G. He, X. Sun, D. Feng, L. Hu, H. Xu, H. Xu, S. Ma and J. Tian, *Nano Res.*, 2020, **13**, 3377–3386.
90 M. A. Cheever and C. S. Higano, *Clin. Cancer Res.*, 2011, **17**, 3520–3526.
91 S. Walter, T. Weinschenk, A. Stenzl, R. Zdrojowy, A. Pluzanska, C. Szczylik, M. Staehler, W. Brugger, P. Dietrich and R. Mendrzyk, *Nature Medicine*, 2012, **18**, 1254–1261.
92 B. Goldman and L. DeFrancesco, *Nat. Biotechnol.*, 2009, **27**, 129–139.
93 C. E. Brown, D. Alizadeh, R. Starr, L. Weng, J. R. Wagner, A. Naranjo, J. R. Ostberg, M. S. Blanchard, J. Kilpatrick and J. Simpson, *N. Engl. J. Med.*, 2016, **375**, 2561–2569.
94 S. S. Neelapu, S. Tummala, P. Kebriaei, W. Wierda, C. Gutierrez, F. L. Locke, K. V. Komanduri, Y. Lin, N. Jain and N. Daver, *Nat. Rev. Clin. Oncol.*, 2018, **15**, 47–62.
95 J. A. Fraietta, S. F. Lacey, E. J. Orlando, I. Pruteanu-Malinici, M. Gohil, S. Lundh, A. C. Boesteanu, Y. Wang, R. S. O Connor and W. Hwang, *Nature Medicine*, 2018, **24**, 563–571.
96 C. H. June, R. S. O Connor, O. U. Kawalekar, S. Ghassemi and M. C. Milone, *Science*, 2018, **359**, 1361–1365.
97 P. Sharma and J. P. Allison, *Science*, 2015, **348**, 56–61.
98 S. L. Topalian, J. M. Taube, R. A. Anders and D. M. Pardoll, *Nat. Rev. Cancer*, 2016, **16**, 275–287.
99 N. Auslander, G. Zhang, J. S. Lee, D. T. Frederick, B. Miao, T. Moll, T. Tian, Z. Wei, S. Madan and R. J. Sullivan, *Nature Medicine*, 2018, **24**, 1545–1549.
100 A. H. Morrison, M. S. Diamond, C. A. Hay, K. T. Byrne and R. H. Vonderheide, *Proc. Natl. Acad. Sci. U. S. A.*, 2020, **117**, 8022–8031.
101 G. Dranoff, *Nat. Rev. Cancer*, 2004, **4**, 11–22.
102 H. Van Gorp and M. Lamkanfi, *EMBO Rep.*, 2019, **20**, e47575.
103 J. Qiao and Y. Fu, *Cell. Mol. Immunol.*, 2020, **17**, 722–727.
104 S. Napolitano, G. Brancaccio, G. Argenziano, E. Martinelli, F. Morgillo, F. Ciardiello and T. Troiani, *Cancer Treat. Rev.*, 2018, **69**, 101–111.
105 N. Kojima, L. Biao, T. Nakayama, M. Ishii, Y. Ikehara and K. Tsujimura, *J. Controlled Release*, 2008, **129**, 26–32.
106 S. Nierkens, M. H. den Brok, Z. Garcia, S. Togher, J. Wagenaars, M. Wassink, L. Boon, T. J. Ruers, C. G. Figdor and S. P. Schoenberger, *Cancer Res.*, 2011, **71**, 6428–6437.
107 R. A. Morgan, J. C. Yang, M. Kitano, M. E. Dudley, C. M. Laurencot and S. A. Rosenberg, *Mol. Ther.*, 2010, **18**, 843–851.
108 P. Sharma and J. P. Allison, *Science*, 2015, **348**, 56–61.
109 C. Wu, K. T. Roybal, E. M. Puchner, J. Onuffer and W. A. Lim, *Science*, 2015, **350**, aab4077.
110 D. S. Chen and I. Mellman, *Immunity*, 2013, **39**, 1–10.
111 I. Melero, D. M. Berman, M. A. Aznar, A. J. Korman, J. L. P. Gracia and J. Haanen, *Nat. Rev. Cancer*, 2015, **15**, 457–472.
112 S. A. Grupp, M. Kalos, D. Barrett, R. Aplenc, D. L. Porter, S. R. Rheingold, D. T. Teachey, A. Chew, B. Hauck and J. F. Wright, *N. Engl. J. Med.*, 2013, **368**, 1509–1518.

113 K. Sato, N. Sato, B. Xu, Y. Nakamura, T. Nagaya, P. L. Choyke, Y. Hasegawa and H. Kobayashi, *Sci. Transl. Med.*, 2016, **8**, 352ra110.
114 S. Yan, Z. Luo, Z. Li, Y. Wang, J. Tao, C. Gong and X. Liu, *Angew. Chem., Int. Ed.*, 2020, **132**, 17484–17495.
115 J. Xiang, L. Xu, H. Gong, W. Zhu, C. Wang, J. Xu, L. Feng, L. Cheng, R. Peng and Z. Liu, *ACS Nano*, 2015, **9**, 6401–6411.
116 H. Chu, J. Zhao, Y. Mi, Z. Di and L. Li, *Nat. Commun.*, 2019, **10**, 2839.
117 Z. Wang, Q. Han, X. Zhao, X. Xie, Z. Wang, J. Lin and B. Xing, *J. Controlled Release*, 2020, **324**, 104–123.
118 A. P. Castano, P. Mroz and M. R. Hamblin, *Nat. Rev. Cancer*, 2006, **6**, 535–545.
119 B. Ding, S. Shao, C. Yu, B. Teng, M. Wang, Z. Cheng, K. L. Wong, P. Ma and J. Lin, *Adv. Mater.*, 2018, **30**, 1802479.
120 W. Song, J. Kuang, C. Li, M. Zhang, D. Zheng, X. Zeng, C. Liu and X. Zhang, *ACS Nano*, 2018, **12**, 1978–1989.
121 K. Lu, C. He, N. Guo, C. Chan, K. Ni, G. Lan, H. Tang, C. Pelizzari, Y. Fu and M. T. Spiotto, *Nat. Biomed. Eng.*, 2018, **2**, 600–610.
122 K. Lu, C. He, N. Guo, C. Chan, K. Ni, R. R. Weichselbaum and W. Lin, *J. Am. Chem. Soc.*, 2016, **138**, 12502–12510.
123 C. Yang, Y. Fu, C. Huang, D. Hu, K. Zhou, Y. Hao, B. Chu, Y. Yang and Z. Qian, *Biomaterials*, 2020, **255**, 120194.
124 J. Xu, L. Xu, C. Wang, R. Yang, Q. Zhuang, X. Han, Z. Dong, W. Zhu, R. Peng and Z. Liu, *ACS Nano*, 2017, **11**, 4463–4474.
125 Y. Shao, B. Liu, Z. Di, G. Zhang, L. Sun, L. Li and C. Yan, *J. Am. Chem. Soc.*, 2020, **142**, 3939–3946.
126 F. Jin, J. Qi, D. Liu, Y. You, G. Shu, Y. Du, J. Wang, X. Xu, X. Ying, J. Ji and Y. Du, *J. Controlled Release*, 2021, **337**, 90–104.
127 M. Wang, J. Song, F. Zhou, A. R. Hoover, C. Murray, B. Zhou, L. Wang, J. Qu and W. R. Chen, *Adv. Sci.*, 2019, **6**, 1802157.
128 J. Yan, B. Li, P. Yang, J. Lin and Y. Dai, *Adv. Funct. Mater.*, 2021, 2104325.
129 M. Lin, Y. Gao, F. Hornicek, F. Xu, T. J. Lu, M. Amiji and Z. Duan, *Adv. Colloid Interface Sci.*, 2015, **226**, 123–137.
130 W. Lai, A. L. Rogach and W. Wong, *Chem. Sci.*, 2017, **8**, 7339–7358.
131 L. Yang, B. Shao, X. Zhang, Q. Cheng, T. Lin and E. Liu, *J. Biomater. Appl.*, 2016, **31**, 400–410.
132 U. Kostiv, I. Kotelnikov, V. Proks, M. Šlouf, J. Kučka, H. Engstová, P. Ježek and D. Horák, *ACS Appl. Mater. Interfaces*, 2016, **8**, 20422–20431.
133 W. Lai, A. L. Rogach and W. Wong, *Chem. Sci.*, 2017, **8**, 7339–7358.
134 S. Jiang, Y. Zhang, K. M. Lim, E. K. Sim and L. Ye, *Nanotechnology*, 2009, **20**, 155101.
135 M. Lin, Y. Gao, T. J. Diefenbach, J. K. Shen, F. J. Hornicek, Y. I. Park, F. Xu, T. J. Lu, M. Amiji and Z. Duan, *ACS Appl. Mater. Interfaces*, 2017, **9**, 7941–7949.
136 L. He, L. Feng, L. Cheng, Y. Liu, Z. Li, R. Peng, Y. Li, L. Guo and Z. Liu, *ACS Appl. Mater. Interfaces*, 2013, **5**, 10381–10388.
137 X. Bai, S. Xu, J. Liu and L. Wang, *Talanta*, 2016, **150**, 118–124.
138 M. K. G. Jayakumar, A. Bansal, B. N. Li and Y. Zhang, *Nanomedicine*, 2015, **10**, 1051–1061.
139 H. Guo, D. Yan, Y. Wei, S. Han, H. Qian, Y. Yang, Y. Zhang, X. Liu and S. Sun, *PLoS One*, 2014, **9**, e112713.
140 S. J. Tan, P. Kiatwuthinon, Y. H. Roh, J. S. Kahn and D. Luo, *Small*, 2011, **7**, 841–856.
141 M. K. G. Jayakumar, A. Bansal, K. Huang, R. Yao, B. N. Li and Y. Zhang, *ACS Nano*, 2014, **8**, 4848–4858.
142 S. W. S. Young, M. Stenzel and Y. Jia-Lin, *Critical Reviews in Oncology Hematology*, 2016, **98**, 159–169.
143 H. K. Karnati, R. S. Yalagala, R. Undi, S. R. Pasupuleti and R. K. Gutti, *Tumor Biol.*, 2014, **35**, 9505–9521.
144 Y. He, S. Guo, L. Wu, P. Chen, L. Wang, Y. Liu and H. Ju, *Biomaterials*, 2019, **225**, 119501.
145 Y. Zhang, K. Ren, X. Zhang, Z. Chao, Y. Yang, D. Ye, Z. Dai, Y. Liu and H. Ju, *Biomaterials*, 2018, **163**, 55–66.
146 M. Lin, Y. Gao, T. J. Diefenbach, J. K. Shen, F. J. Hornicek, Y. I. Park, F. Xu, T. J. Lu, M. Amiji and Z. Duan, *ACS Appl. Mater. Interfaces*, 2017, **9**, 7941–7949.
147 V. T. DeVita and E. Chu, *Cancer Res.*, 2008, **68**, 8643–8653.
148 X. Ma and Z. Wang, *Drug Discovery Today*, 2009, **14**, 1136–1142.
149 B. Fu, N. Wang, H. Tan, S. Li, F. Cheung and Y. Feng, *Front. Pharmacol.*, 2018, **9**, 1394.
150 J. H. Atkins and L. J. Gershell, *Nat. Rev. Cancer*, 2002, **1**, 645–646.
151 D. J. Irvine, *Nat. Mater.*, 2011, **10**, 342–343.
152 J. A. Hubbell and R. Langer, *Nat. Mater.*, 2013, **12**, 963–966.
153 S. Mura, J. Nicolas and P. Couvreur, *Nat. Mater.*, 2013, **12**, 991–1003.
154 R. Mahato, W. Tai and K. Cheng, *Adv. Drug Delivery Rev.*, 2011, **63**, 659–670.
155 M. E. Davis, Z. Chen and D. M. Shin, *Nat. Rev. Drug Discovery*, 2008, **7**, 771–782.
156 O. C. Farokhzad and R. Langer, *ACS Nano*, 2009, **3**, 16–20.
157 Y. Chen, S. Liu, Z. Hou, P. Ma, D. Yang, C. Li and J. Lin, *Nano Res.*, 2015, **8**, 1917–1931.
158 H. Li, R. Wei, G. Yan, J. Sun, C. Li, H. Wang, L. Shi, J. A. Capobianco and L. Sun, *ACS Appl. Mater. Interfaces*, 2018, **10**, 4910–4920.
159 Q. Chen, M. Chen and Z. Liu, *Chem. Soc. Rev.*, 2019, **48**, 5506–5526.
160 Z. Xie, T. Fan, J. An, W. Choi, Y. Duo, Y. Ge, B. Zhang, G. Nie, N. Xie and T. Zheng, *Chem. Soc. Rev.*, 2020, **49**, 8056–8087.
161 N. Zhao, B. Wu, X. Hu and D. Xing, *Biomaterials*, 2017, **141**, 40–49.
162 J. Du, L. A. Lane and S. Nie, *J. Controlled Release*, 2015, **219**, 205–214.
163 Y. Wang, Y. Deng, H. Luo, A. Zhu, H. Ke, H. Yang and H. Chen, *ACS Nano*, 2017, **11**, 12134–12144.
164 W. Fan, B. C. Yung and X. Chen, *Angew. Chem., Int. Ed.*, 2018, **57**, 8383–8394.
165 Y. Qiao, J. Wan, L. Zhou, W. Ma, Y. Yang, W. Luo, Z. Yu and H. Wang, *Wiley Interdiscip. Rev.: Nanomed. Nanobiotechnol.*, 2019, **11**, e1527.

166 B. Chen, W. Dai, B. He, H. Zhang, X. Wang, Y. Wang and Q. Zhang, *Theranostics*, 2017, **7**, 538–558.
167 N. Zhao, B. Wu, X. Hu and D. Xing, *Biomaterials*, 2017, **141**, 40–49.
168 M. Xu, G. Yang, H. Bi, J. Xu, S. Dong, T. Jia, Z. Wang, R. Zhao, Q. Sun and S. Gai, *Chem. Eng. J.*, 2020, **382**, 122822.
169 B. Teng, B. Ding, S. Shao, Z. Wang, W. Tong, S. Wang, Z. Cheng, J. Lin and P. Ma, *Chem. Eng. J.*, 2021, **405**, 126606.
170 G. Tian, Z. Gu, L. Zhou, W. Yin, X. Liu, L. Yan, S. Jin, W. Ren, G. Xing and S. Li, *Adv. Mater.*, 2012, **24**, 1226–1231.
171 Y. Dai, H. Xiao, J. Liu, Q. Yuan, P. A. Ma, D. Yang, C. Li, Z. Cheng, Z. Hou and P. Yang, *J. Am. Chem. Soc.*, 2013, **135**, 18920–18929.
172 C. Carling, J. Boyer and N. R. Branda, *J. Am. Chem. Soc.*, 2009, **131**, 10838–10839.
173 J. Yu, W. Yin, T. Peng, Y. Chang, Y. Zu, J. Li, X. He, X. Ma, Z. Gu and Y. Zhao, *Nanoscale*, 2017, **9**, 4497–4507.
174 K. Wang, J. Ma, M. He, G. Gao, H. Xu, J. Sang, Y. Wang, B. Zhao and D. Cui, *Theranostics*, 2013, **3**, 258–266.
175 L. Xiong, T. Yang, Y. Yang, C. Xu and F. Li, *Biomaterials*, 2010, **31**, 7078–7085.
176 C. Liu, Y. Hou and M. Gao, *Adv. Mater.*, 2014, **26**, 6922–6932.
177 A. Gnach, T. Lipinski, A. Bednarkiewicz, J. Rybka and J. A. Capobianco, *Chem. Soc. Rev.*, 2015, **44**, 1561–1584.